Extending a Galaxy Cluster Population Model to Group-scale Masses

A Story of Baryonic Component Covariance

Trevor Ponman
@Schloss Ringberg
2003

August (Gus) Evrard

Arthur F. Thurnau Professor
Departments of Physics and Astronomy
Michigan Center for Theoretical Physics
University of Michigan

Collaborators

- X-ray follow-up of DES clusters


Devon Hollowood +
Tesla Jeltema (UCSC)


Alberto Bermeo +
Kathy Romer (Sussex)


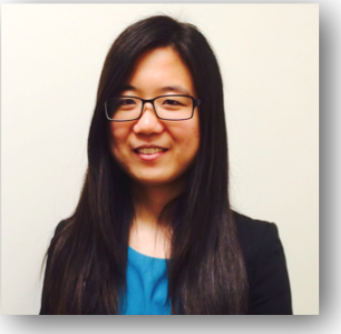

Arya Farahi + Xinyi Chen (Michigan)

THE DARK ENERGY SURVEY

SDSS

- property scaling relations and covariance (LoCuSS + Bahamas/MACSIS)


Sarah Mulroy + Graham Smith (Birmingham)
LoCuSS


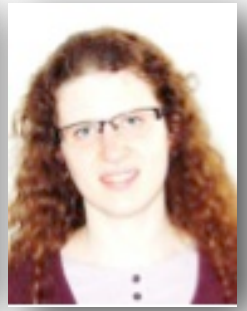

Ian McCarthy (LJMU) +
Amandine Le Brun (Saclay)
Bahamas


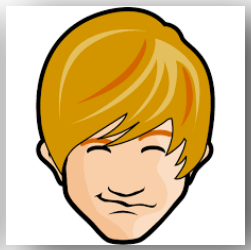

Scott Kay + David Barnes
(Manchester)
MACSIS

outline

- analytical model for **multi-property counts** of massive halos
  Swiss army knife for interpreting sample behavior

- Bahamas+MACSIS simulations
  log-normal form of mass-observable (MOR) PDFs
  running of slope and scatter with mass
  open (groups) to **~closed** (clusters) "baryon box" behavior

- LoCuSS sample observations
  evidence of closed baryon box nature for massive clusters

- X-ray analysis of DES+SDSS redMaPPer samples (preliminary)
  ~log-normal PDFs with sample size approaching 10^3

a model for multi-property cluster counts

Evrard, Arnault, Huterer, Farahi 2014

simple idea: shape of the mass function is **~polynomial** in log-space

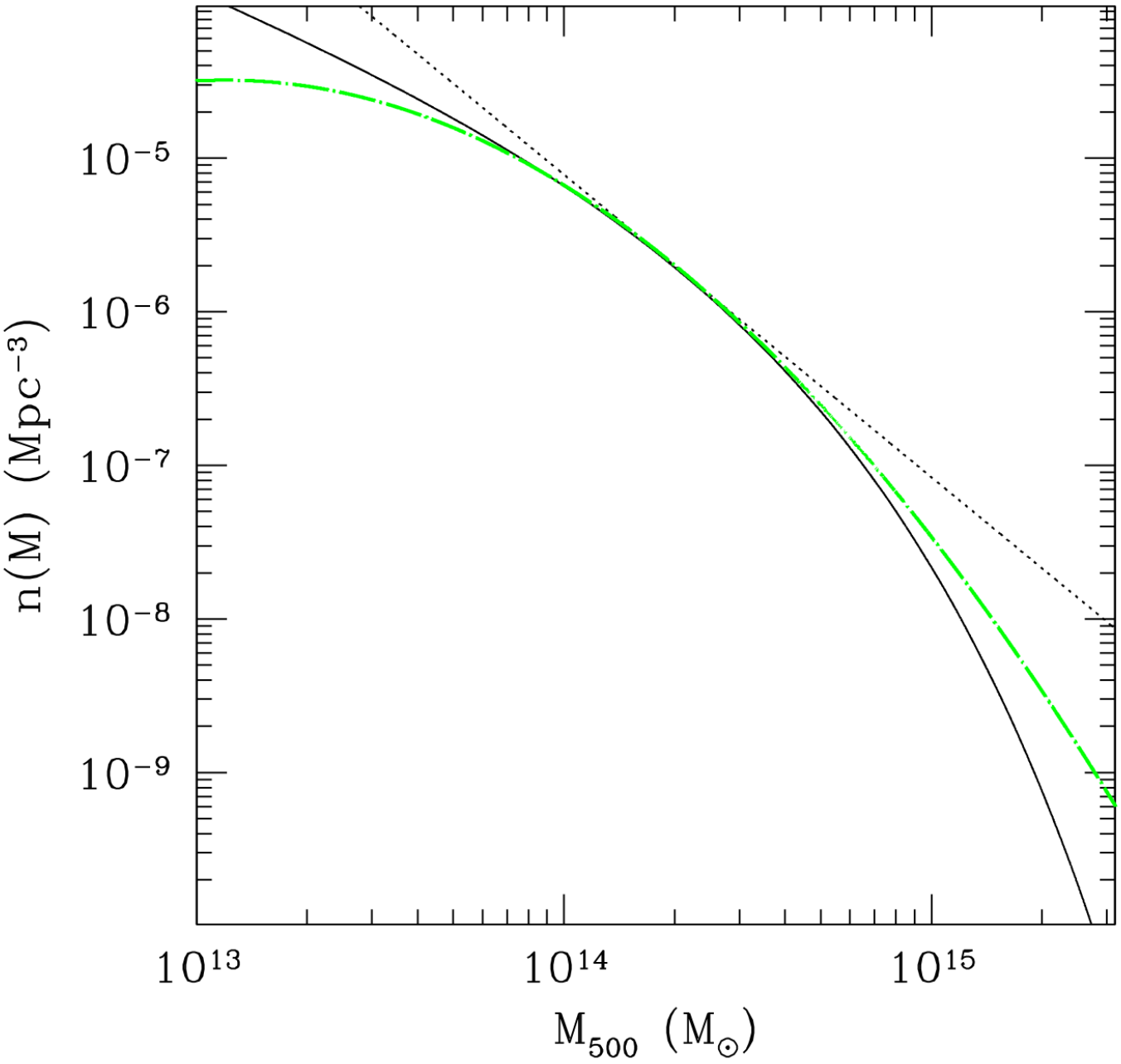

Tinker MF (z=0.2)

log-quadratic

(running power-law)

$$\log(n_1(M)) = \log(A) - \beta_1 \log(M/M_p) - \beta_2/2\,(\log(M/M_p))^2$$

pivot mass:

M_p=2e14 M_{sun}

simple idea: shape of the mass function is **~polynomial** in log-space

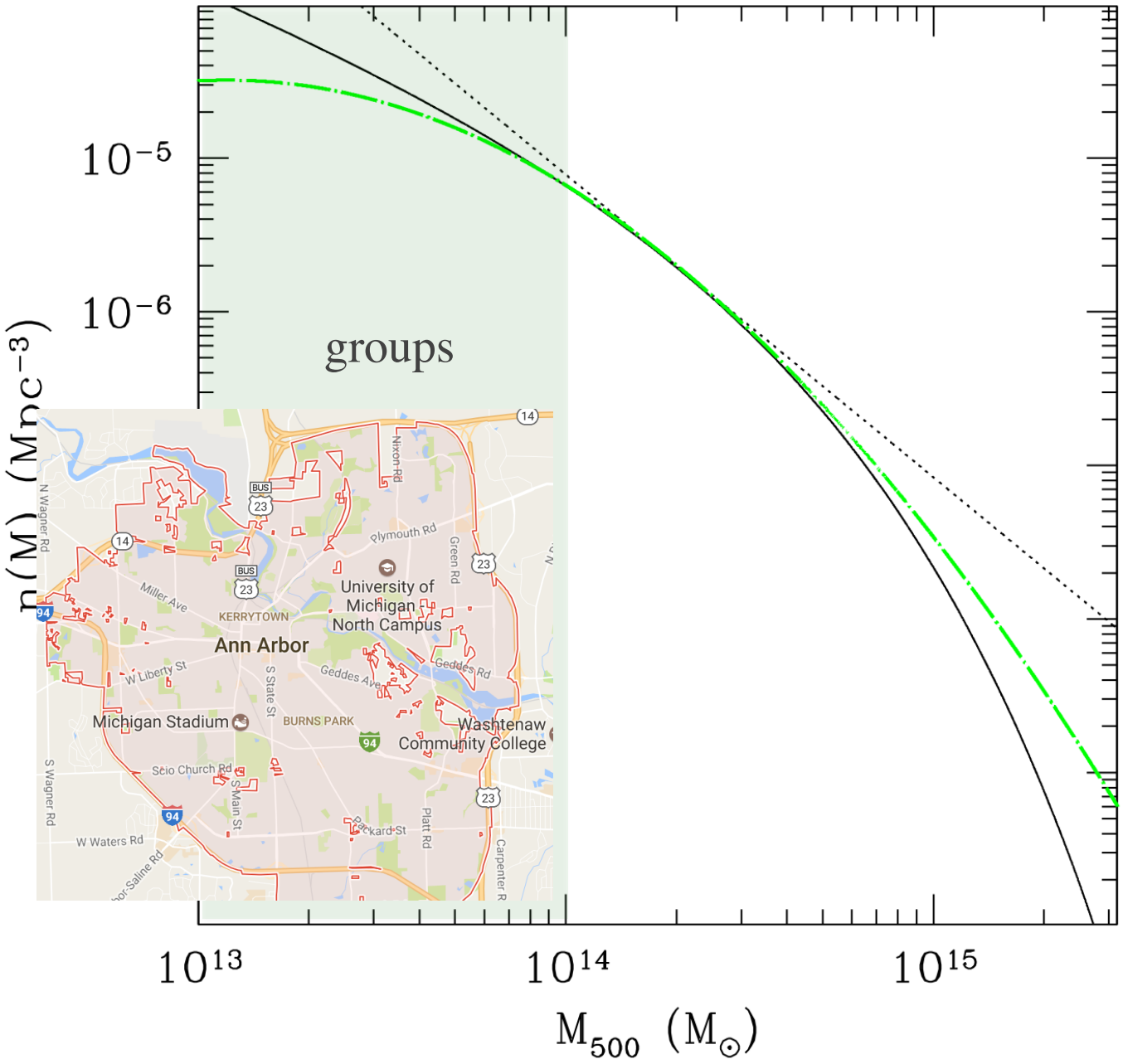

Tinker MF (z=0.2)

log-quadratic

(running power-law)

$$\log(n_1(M)) = \log(A) - \beta_1 \log(M/M_p) - \beta_2/2\,(\log(M/M_p))^2$$

pivot mass:

M_p=2e14 M_{sun}

simple idea: shape of the mass function is **~polynomial** in log-space

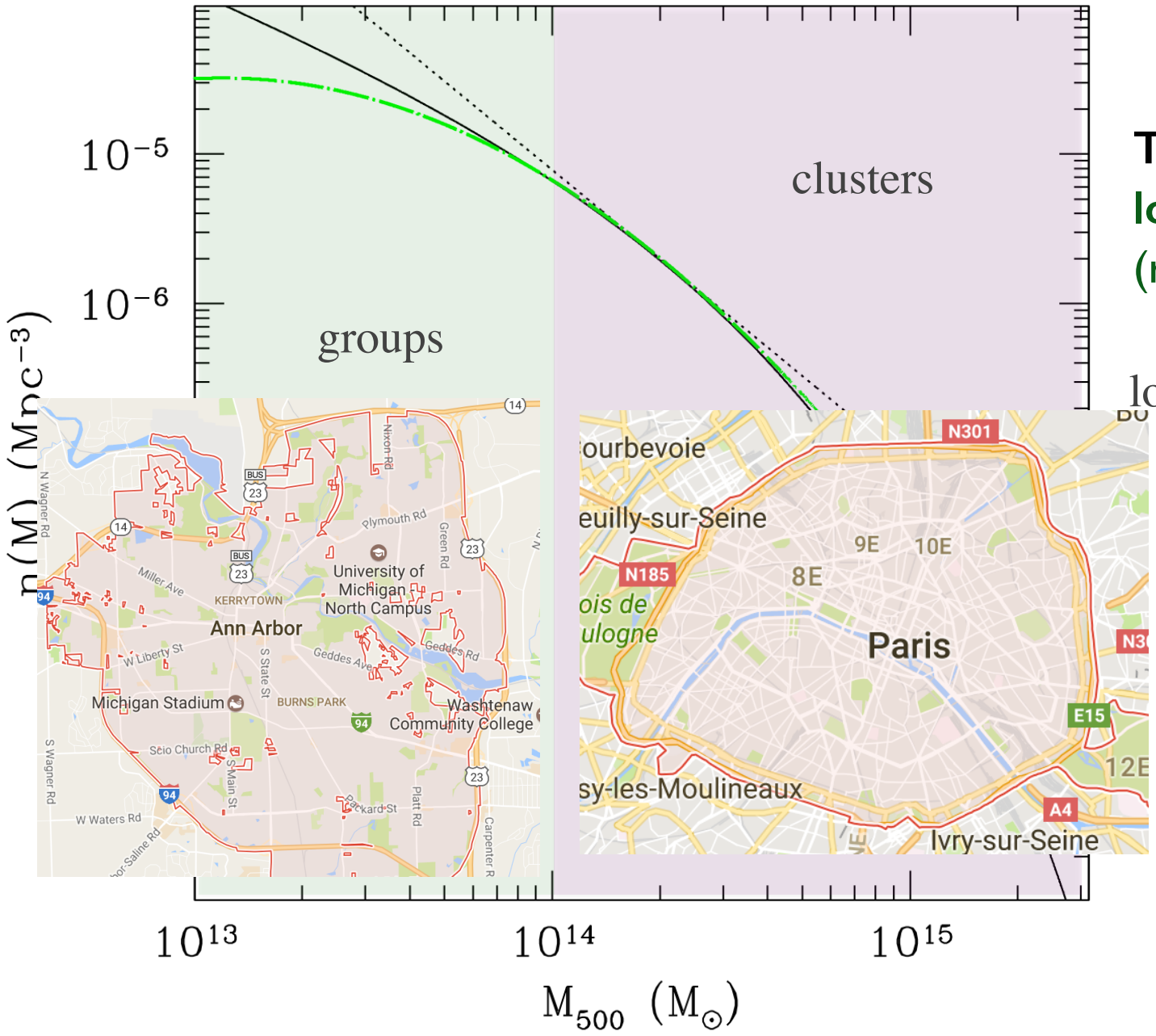

Tinker MF (z=0.2)

log-quadratic

(running power-law)

$$\log(n_1(M)) = \log(A) - \beta_1 \log(M/M_p) - \beta_2/2\,(\log(M/M_p))^2$$

pivot mass:

M_p=2e14 M_{sun}

X-ray luminosity functions from polynomial (log) mass function

MOR convolution takes **analytic form**

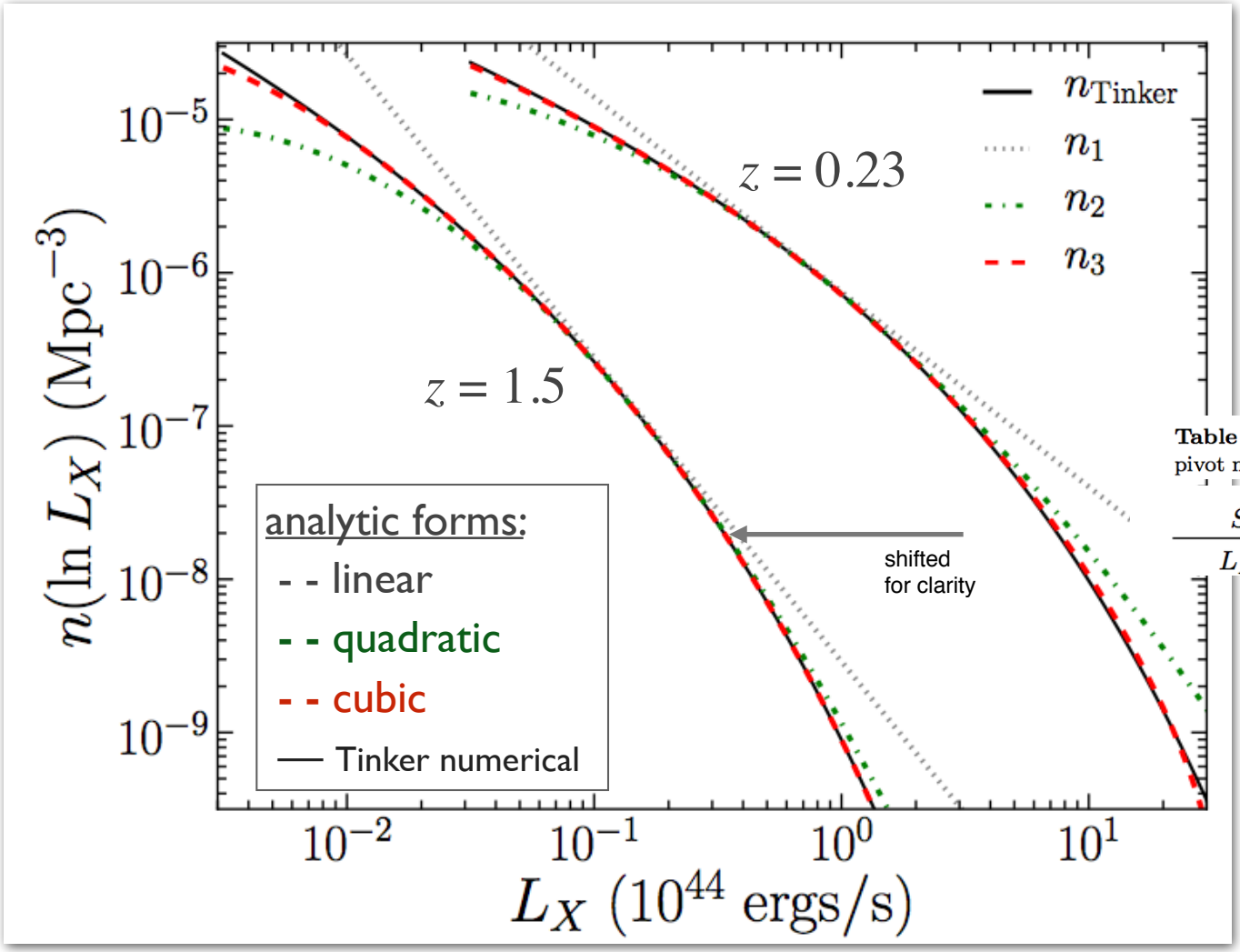

MF data from HMFcalc

Murray et al (2013)

z	M_p	A	β_1	β_2	β_3
0.23	2.0	1.944	1.97	0.70	0.40
1.5	1.0	0.293	3.07	1.20	0.73

pivot mass, $M_{\rm p}$ (10^{14} $M_{\rm solar}$)

pivot normalization, A (10^{-6} Mpc^{-3})

Table 2. Observable-mass scaling parameters at $z = 0.23$ and pivot mass, $M_p = 2 \times 10^{14} M_\odot$, from Rozo et al. (2014c).

S	$S_p = e^{\pi_s}$	α_s	$\sigma_{\ln S}$	$\sigma_{\mu\|s}$
L_X	0.61	1.55	0.39	0.252

notation…

Evrard et al 2014

scaling relation inputs:

$$\langle \mathbf{s}|\mu\rangle = \boldsymbol{\pi} + \boldsymbol{\alpha}\mu$$ log-means (vector)

$$C_{ab} = \langle (s_a - \langle s_a|\mu\rangle)(s_b - \langle s_b|\mu\rangle)\rangle$$ covariance of log-observables deltas

joint, multi-observable space density

$\mu = \ln M$

$s_i = \ln(\text{observable}_i)$

$$n_1(\mathbf{s}) = A_1' \exp\left[-\frac{1}{2}\left((\mathbf{s}-\boldsymbol{\pi})^T\mathbf{C}^{-1}(\mathbf{s}-\boldsymbol{\pi}) - \frac{\langle\mu|\mathbf{s}\rangle_1^2}{\sigma^2_{\mu|\mathbf{s},1}}\right)\right]$$

$$A_1' = A\,\sigma_{\mu|\mathbf{s},1}\,\left((2\pi)^{N-1}|\mathbf{C}|\right)^{-1/2}$$

$$\langle\mu|\mathbf{s}\rangle_1 = \left[\boldsymbol{\alpha}^T\mathbf{C}^{-1}(\mathbf{s}-\boldsymbol{\pi}) - \beta_1\right]\sigma^2_{\mu|\mathbf{s},1}$$

mean selected mass

$$\sigma^2_{\mu|\mathbf{s},1} = (\boldsymbol{\alpha}^T\mathbf{C}^{-1}\boldsymbol{\alpha})^{-1}.$$

variance in selected mass

scaling behavior of property-selected samples Evrard et al 2014

log-normal pdf, $\mathbf{Pr}(s_b \mid s_a)$, of property-selected samples

$$\langle s_b|s_a\rangle_1 = \pi_b + \alpha_b[\,\langle\mu|s_a\rangle_1 + \beta_1\, r_{ab}\,\sigma_{\mu|a,1}\,\sigma_{\mu|b,1}\,]$$

mean s_b for s_a selection

$$\sigma^2_{b|a,1} = \alpha_b^2\,[\,\sigma^2_{\mu|a,1} + \sigma^2_{\mu|b,1} - 2r_{ab}\,\sigma_{\mu|a,1}\sigma_{\mu|b,1}\,]$$

variance ”

$\mu = \ln M$

$s_i = \ln(\text{property}_i)$

These are what we actually measure in survey samples.

Bahamas+MACSIS simulations: scaling relations & hot-cold baryon covariance

should cold and hot mass fractions anti-correlate in halos?

$$f_{\rm gas} + f_{\rm star} \cong C(=\Omega_b / \Omega_m)$$

$$\Rightarrow \delta f_{\rm gas} \cong -\delta f_{\rm star}$$

"closed box"

$$f_{\rm gas} + f_{\rm star} \cong f_{\rm retain} C$$

$$\Rightarrow \delta f_{\rm gas} + \delta f_{\rm star} = \delta f_{\rm retain}$$

"open box"

Rhapsody-G simulations: cold and hot phase mass anti-correlate

Wu et al 2015

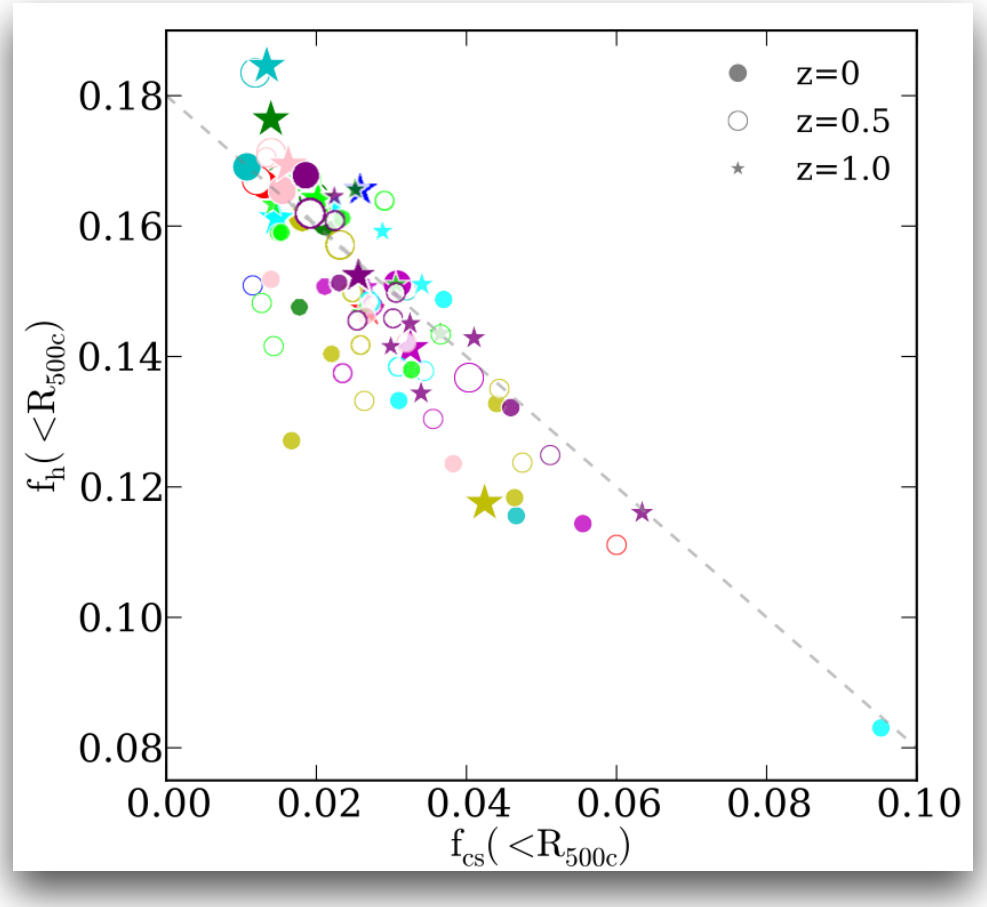

hot gas mass fraction

stellar and cold gas mass fraction

Anti-correlated behavior in mass cold/hot mass fractions

massive (RAMSES) halos are approximately "closed boxes"

Baryon fraction is a lower scatter mass proxy (4.7% in ln*M) than either* f_{gas} *(8%) or* f_{star} *(34%) alone.*

recent comparison of different "full physics" numerical methods (single halo)

Sembolini et al 2016

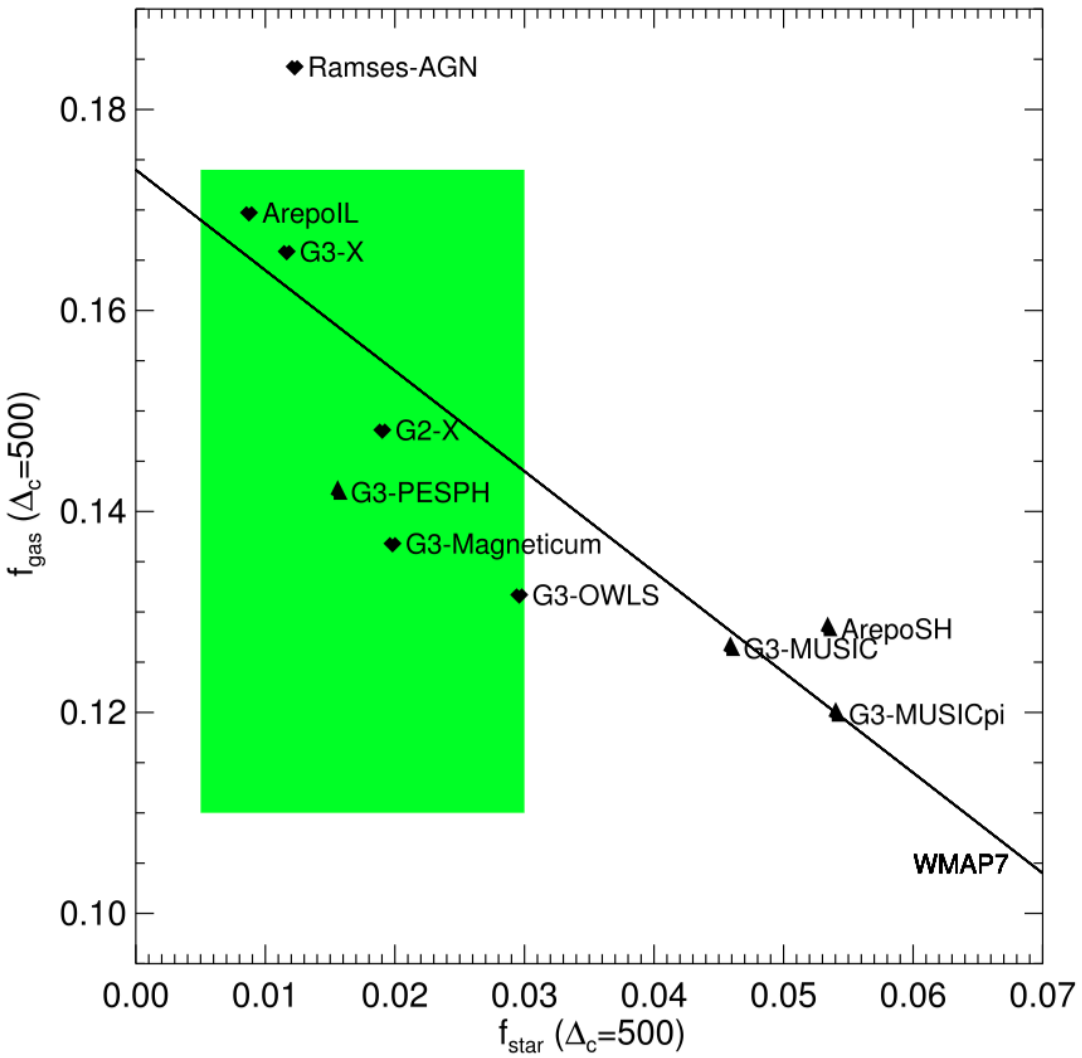

Figure 1. Values of f_{gas} and f_{star} as calculated at $\Delta_c = 500$ for the different codes. The green area corresponds to the phase space supported by observations. Codes including AGN feedback are represented as diamonds, codes not including AGN feedback as triangles. The diagonal line shows the relation $f_{gas}+f_{star} = 0.174$, the value of the cosmic ratio according to *WMAP7*.

Bahamas + MACSIS simulations w/ AGN feedback

McCarthy et al 2016
Barnes et al 2016

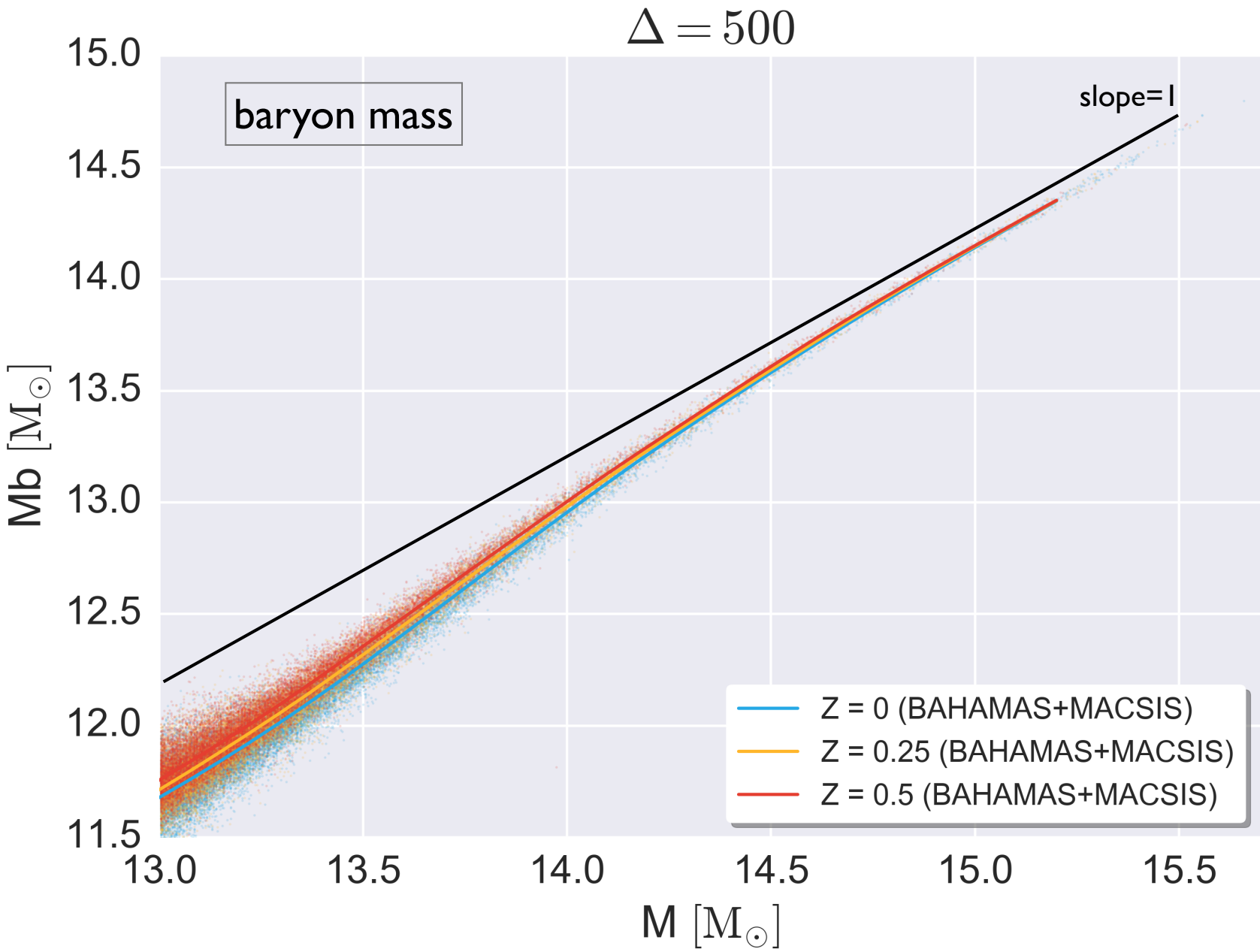

Bahamas + MACSIS simulations w/ AGN feedback

McCarthy et al 2016
Barnes et al 2016

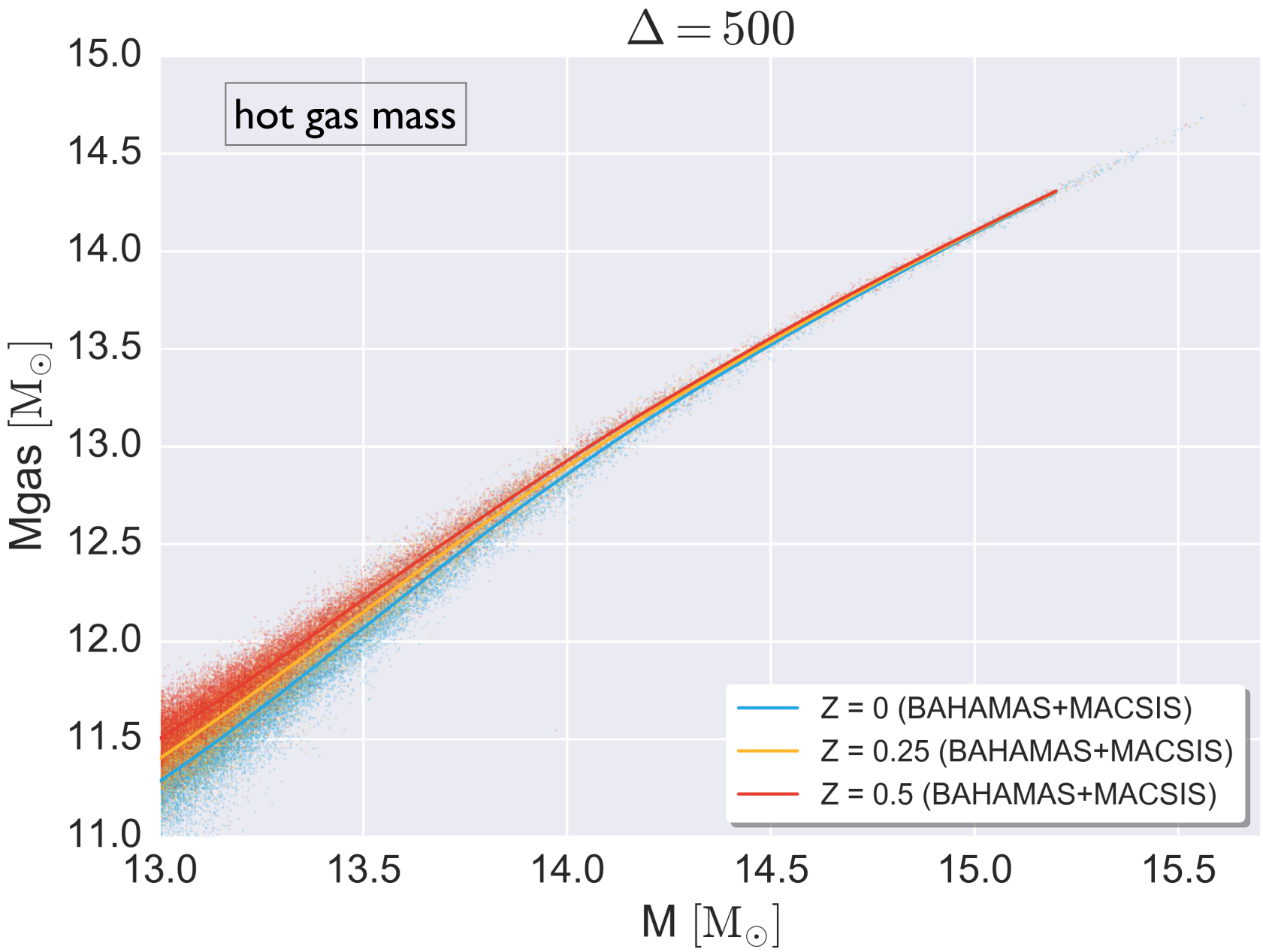

Bahamas + MACSIS simulations w/ AGN feedback

McCarthy et al 2016
Barnes et al 2016

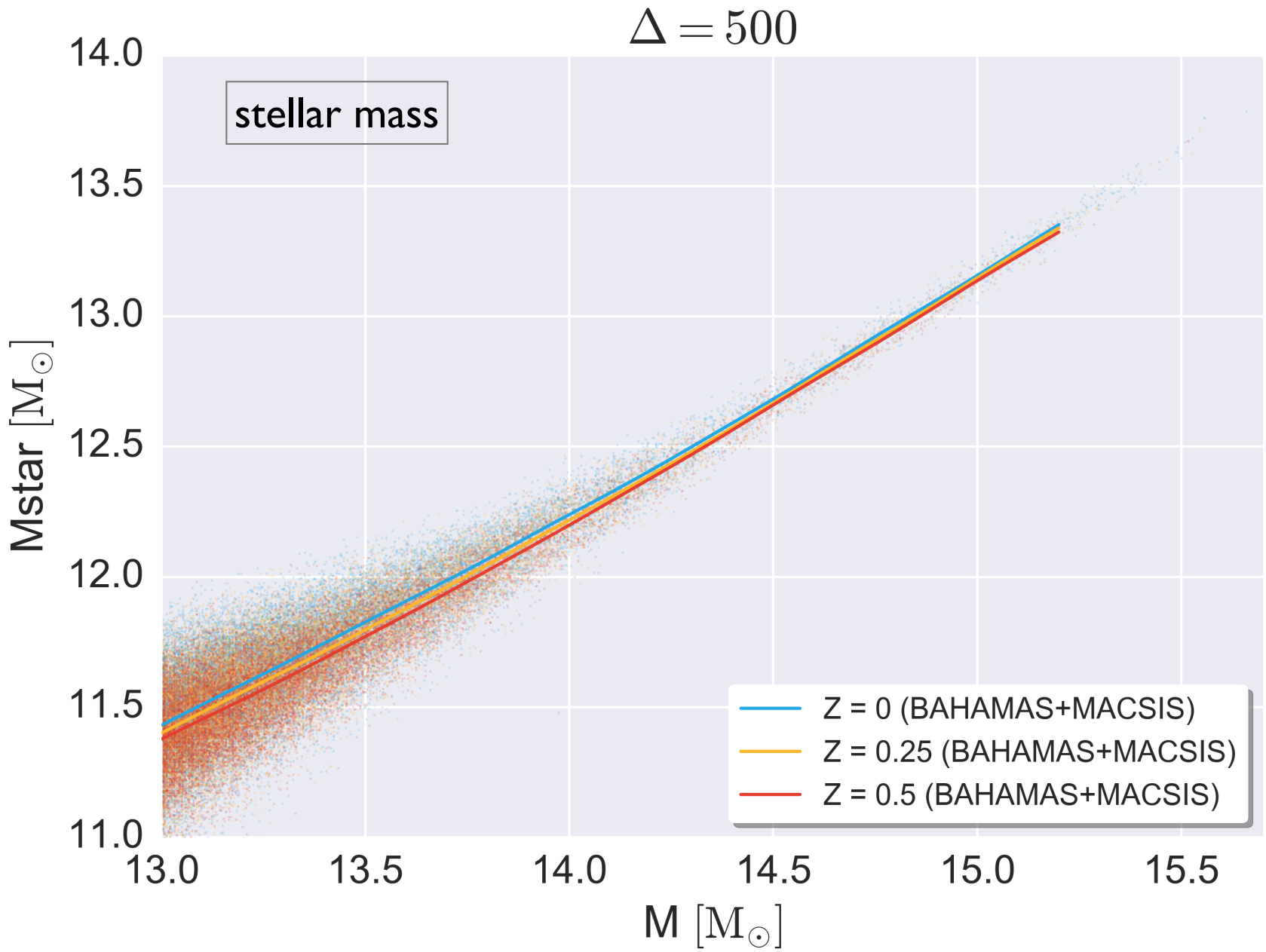

Bahamas + MACSIS simulations w/ AGN feedback

McCarthy et al 2016
Barnes et al 2016

localized, linear regression (0.1 dex gaussian in halo mass)

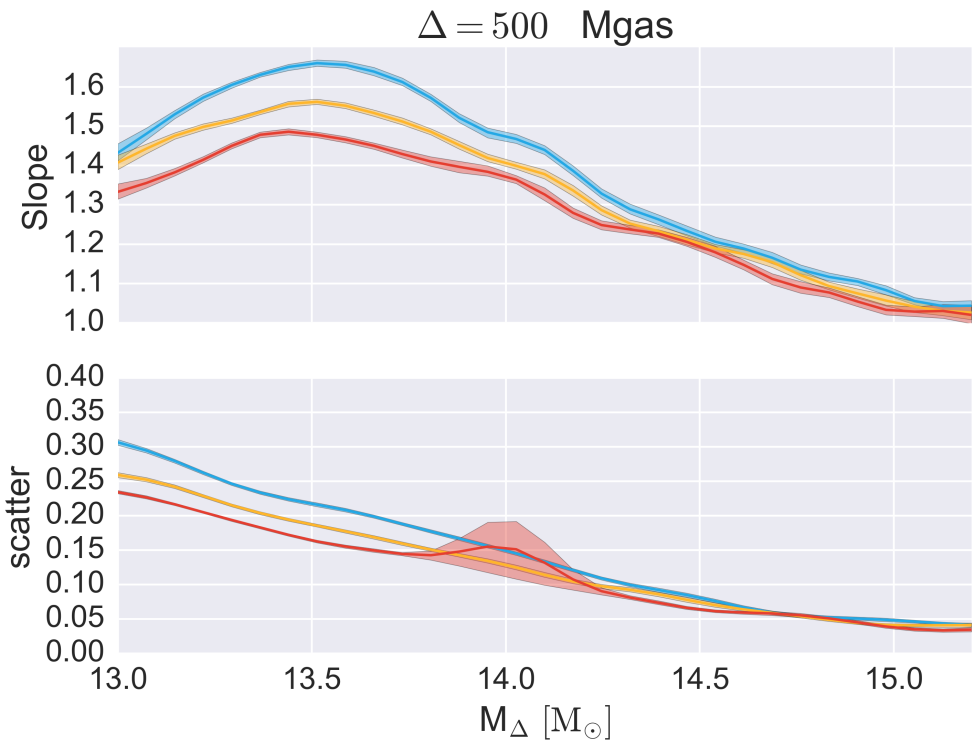

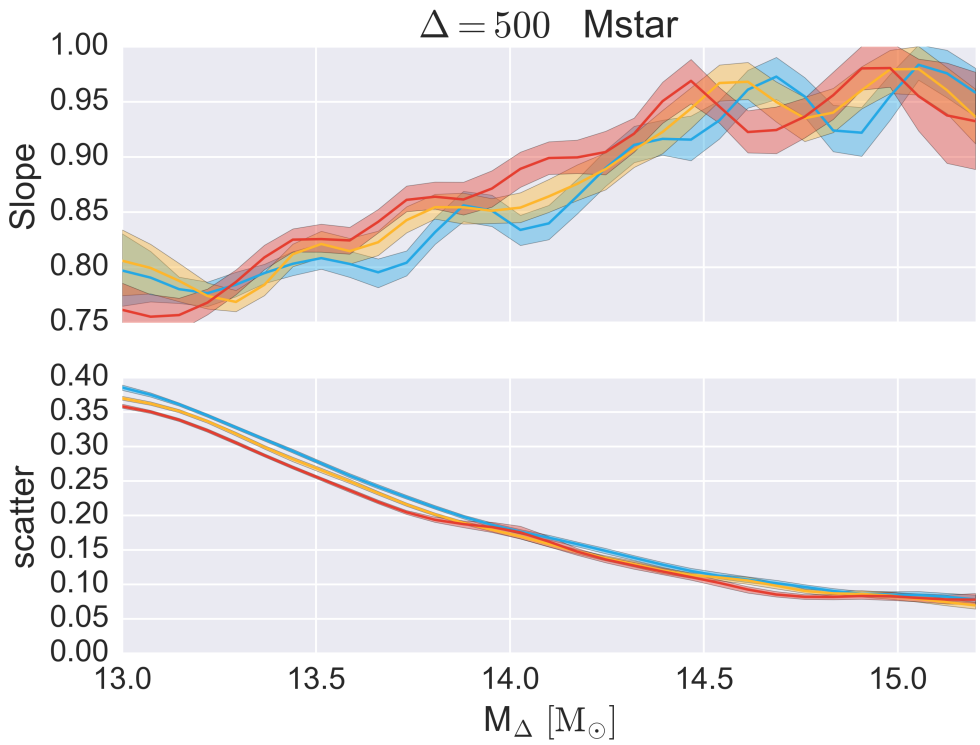

Bahamas + MACSIS simulations w/ AGN feedback

McCarthy et al 2016
Barnes et al 2016

log-normal PDFs of properties around their means

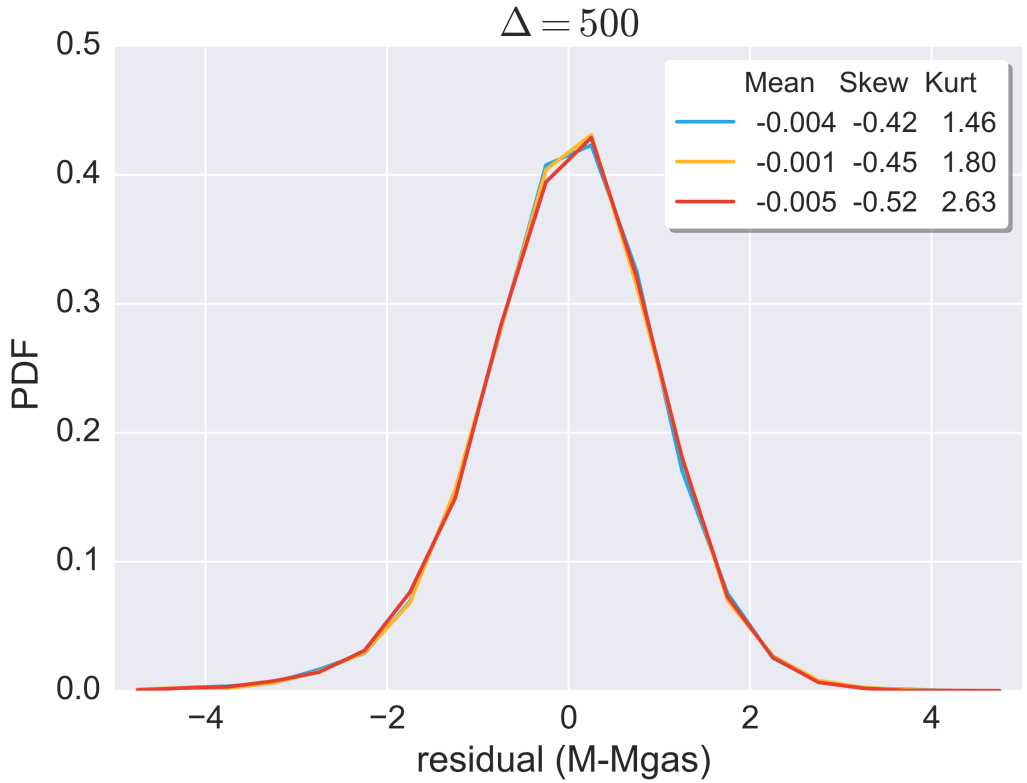

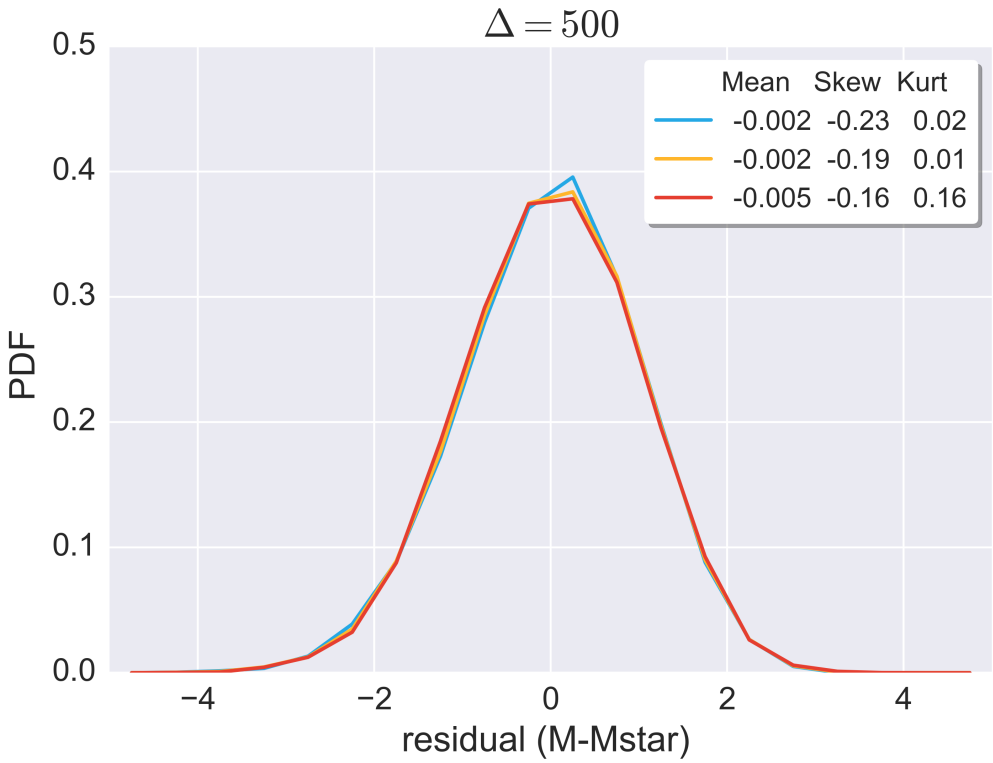

~60,000 halos !

Bahamas + MACSIS simulations w/ AGN feedback

McCarthy et al 2016
Barnes et al 2016

covariance of hot gas + stellar mass at fixed halo mass

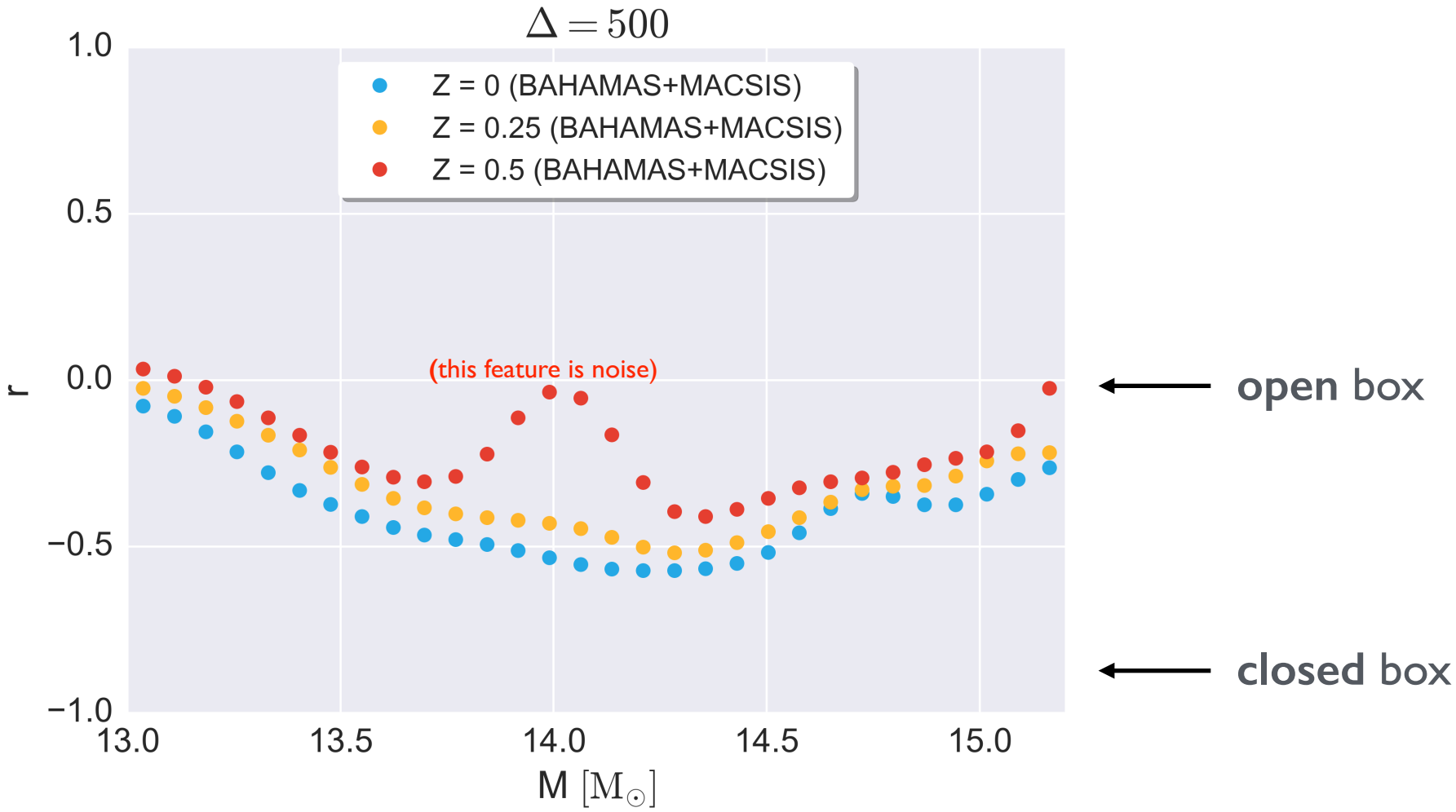

Bahamas + MACSIS simulations w/ AGN feedback

McCarthy et al 2016
Barnes et al 2016

covariance of hot gas + stellar mass at fixed halo mass

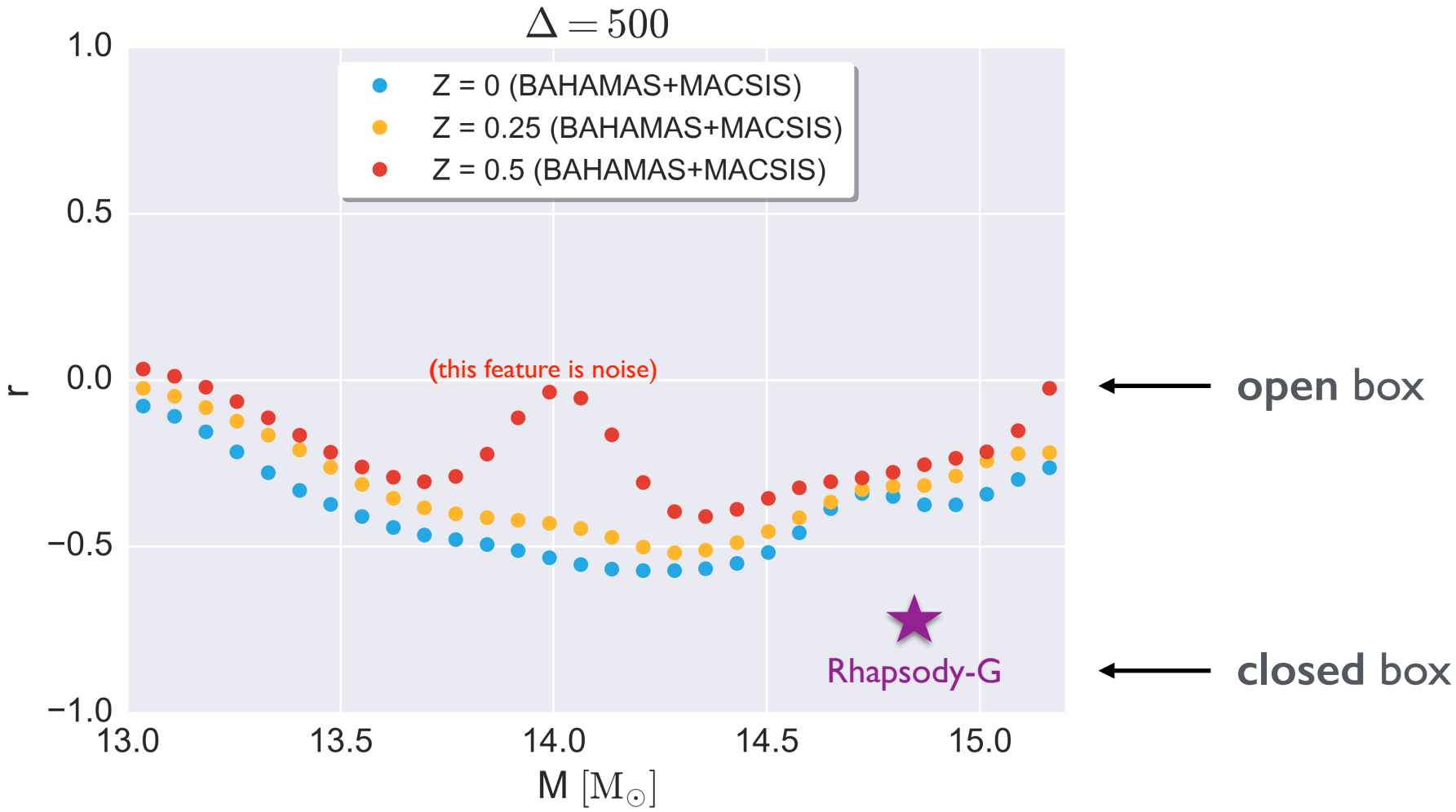

Bahamas + MACSIS simulations: summary

McCarthy et al 2016
Barnes et al 2016

Statistics of ~60k group/cluster halos at low redshift show:

- ~ linear (in logM) **running of slope and scatter** in gas + stellar mass fractions
- log-normal PDF of scatter
- covariance of hot + cold baryon phases trends with mass
  - **groups are ~open** (r ~ 0)
  - **intermediate mass clusters approx. closed** (r ~ –0.5)
  - high mass clusters have r ~ 0 due to very small scatter in each component
    - (tension with Rhapsody-G results*)

* Need observational constraints on intrinsic scatter of baryonic mass in high mass halos.

LoCuSS:
scaling relations &
property covariance

LoCuSS: 42 (RASS-selected) clusters w/ multi-wavelength follow-up

Mulroy, Smith, Farahi et al, in prep.

Hot gas – weak lensing mass relations

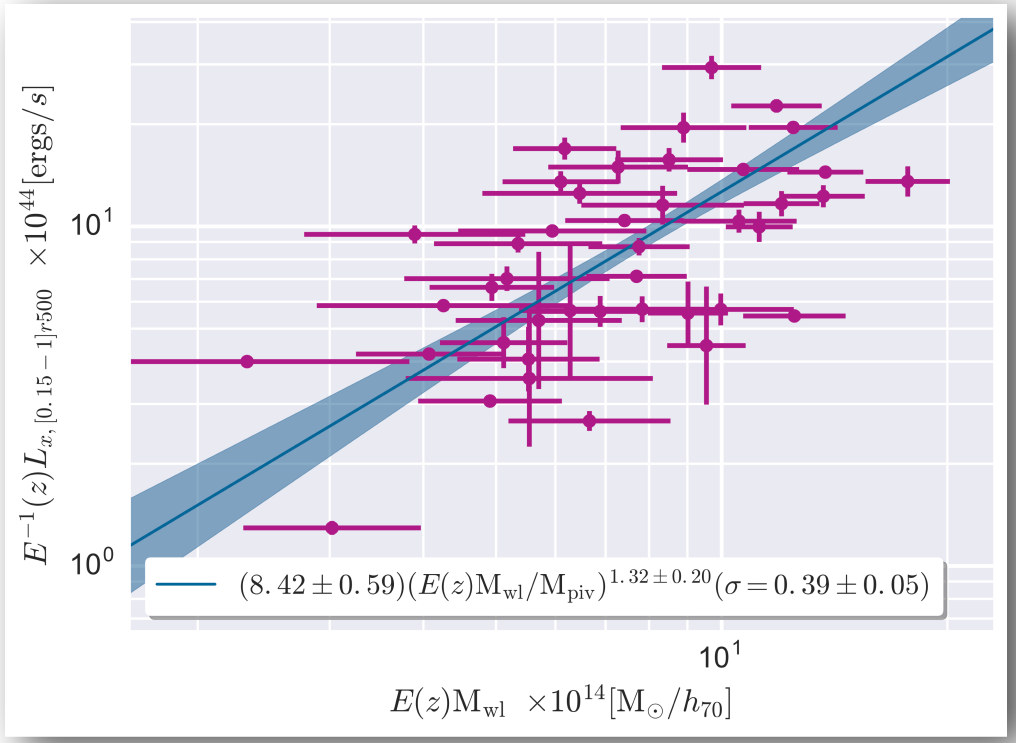

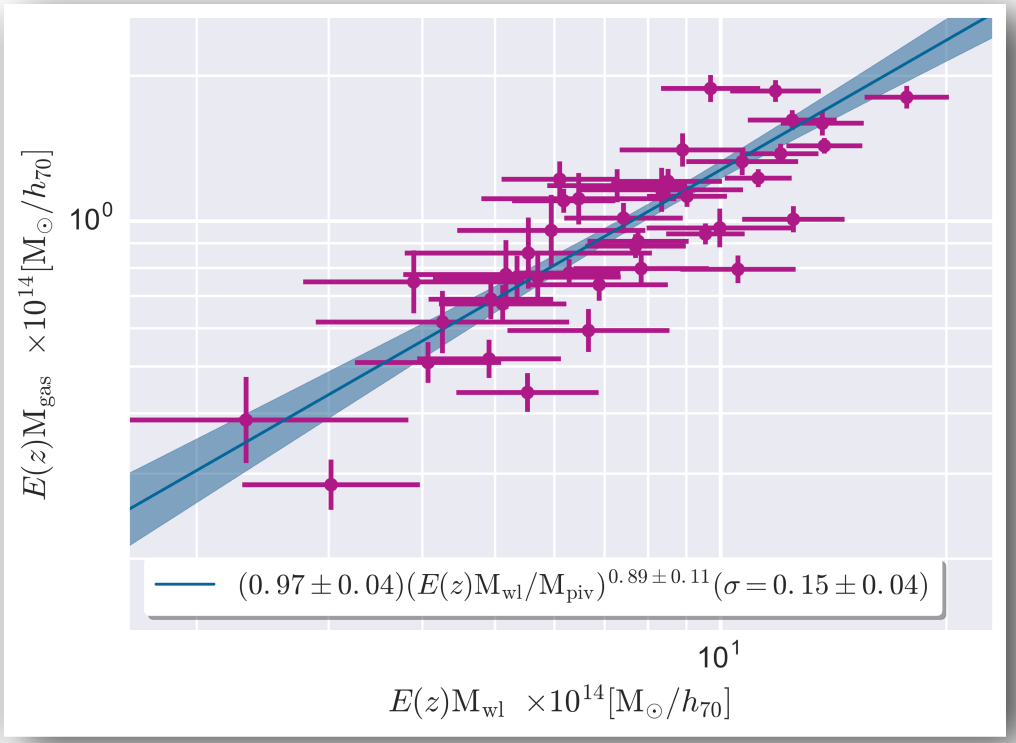

Lx : slope 1.32 ± 0.20
scatter 0.39 ± 0.05

Mgas : slope 0.89 ± 0.11
scatter 0.15 ± 0.04

LoCuSS: 42 (RASS-selected) clusters w/ multi-wavelength follow-up

Hot gas – weak lensing mass relations

Mulroy, Farahi et al, in prep.

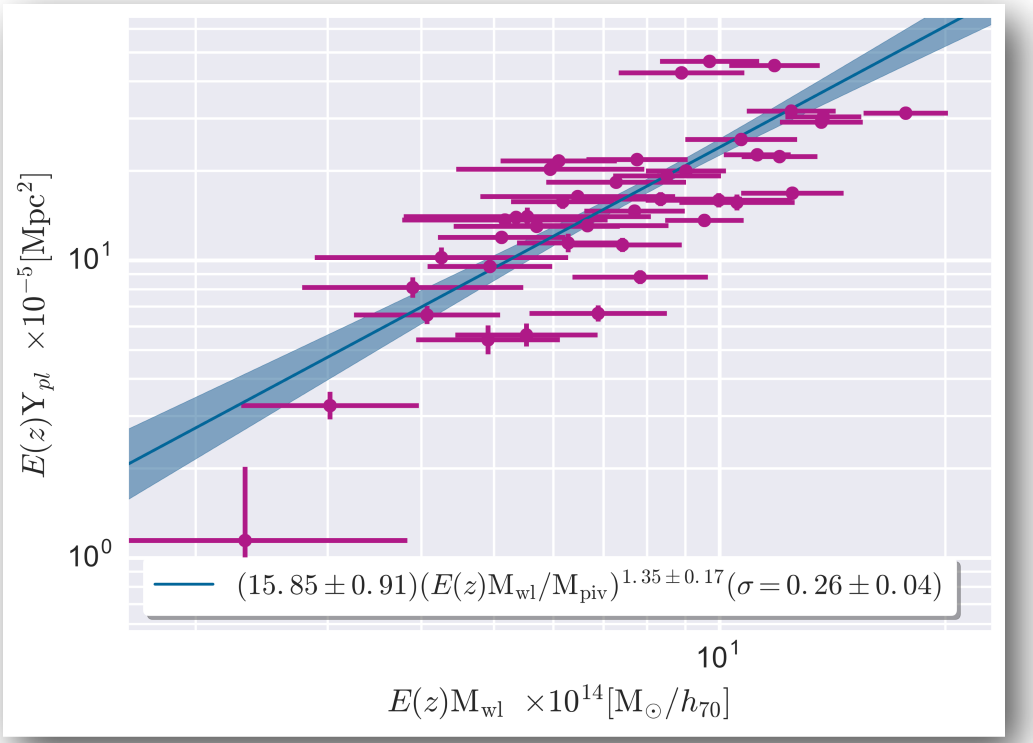

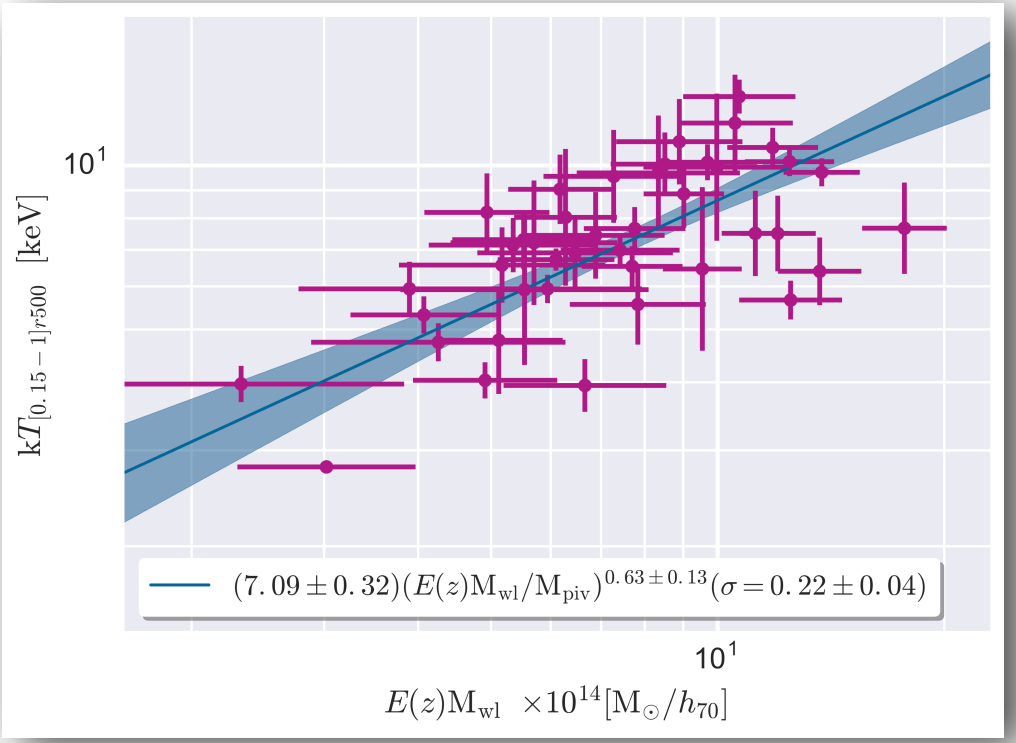

Ypl : slope 1.35 ± 0.17
scatter 0.26 ± 0.04

kT : slope 0.63 ± 0.13
scatter 0.22 ± 0.04

LoCuSS: 42 (RASS-selected) clusters w/ multi-wavelength follow-up

Galaxy – weak lensing mass relations

Mulroy, Farahi et al, in prep.

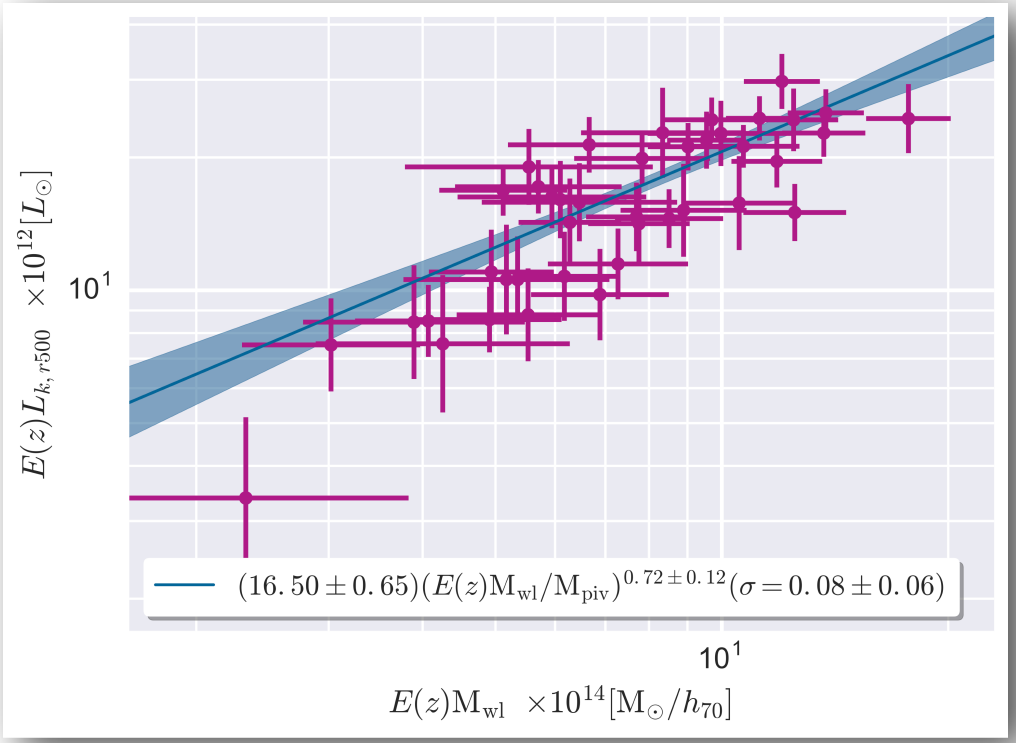

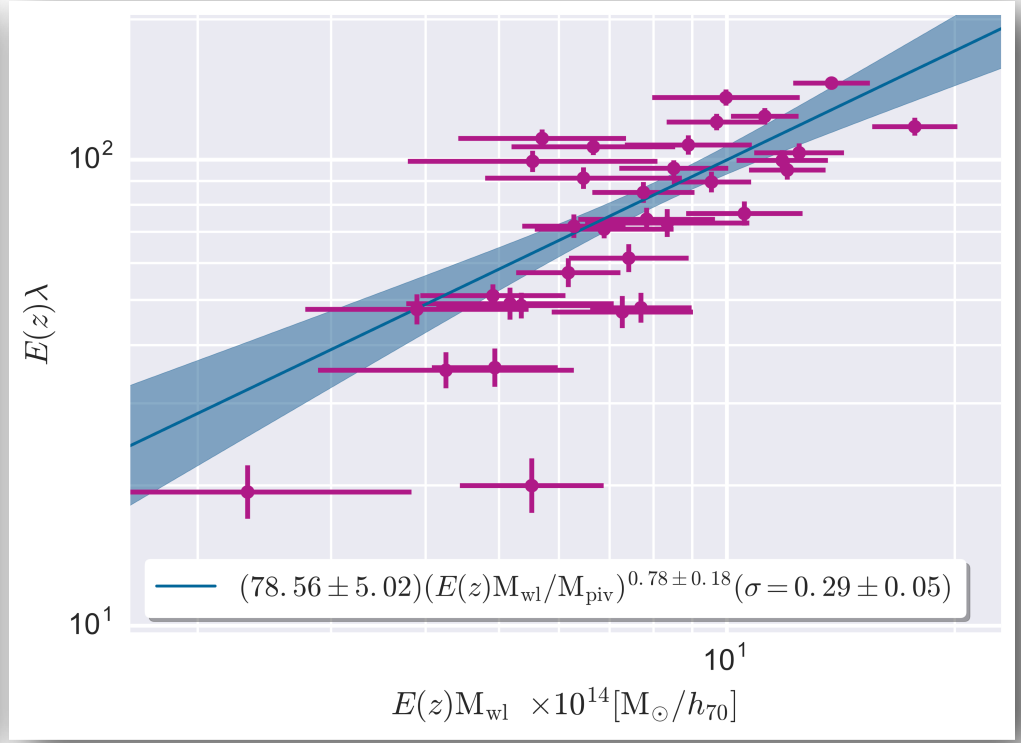

Lk : slope 0.72 ± 0.12
scatter 0.08 ± 0.06

λ : slope 0.78 ± 0.18
scatter 0.29 ± 0.05

see Mulroy et al (2014)

off-diagonal correlation coefficients

Mulroy, Farahi et al, in prep.

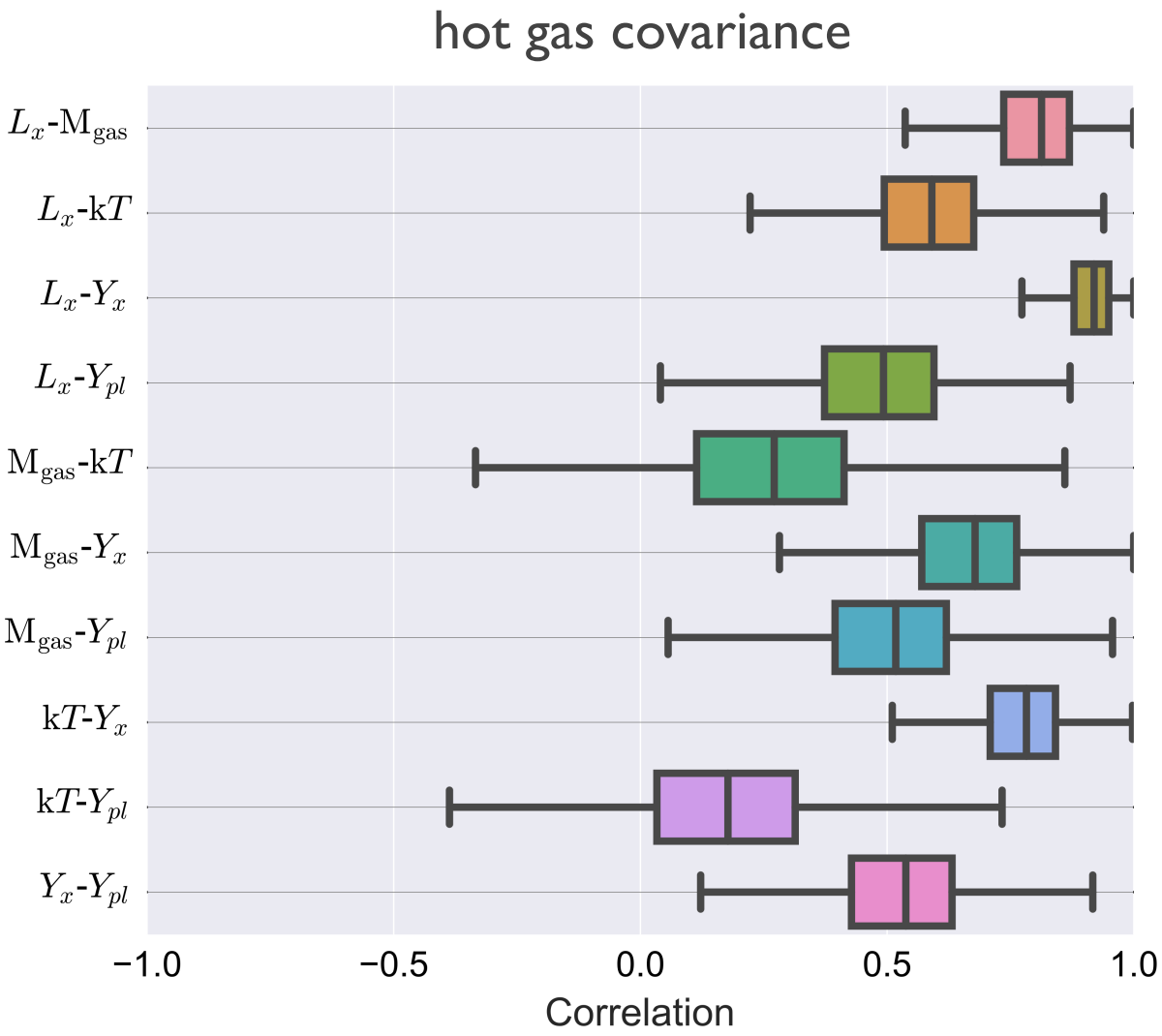

mostly positive correlations (see Mantz et al 2016)

off-diagonal correlation coefficients

Mulroy, Farahi et al, in prep.

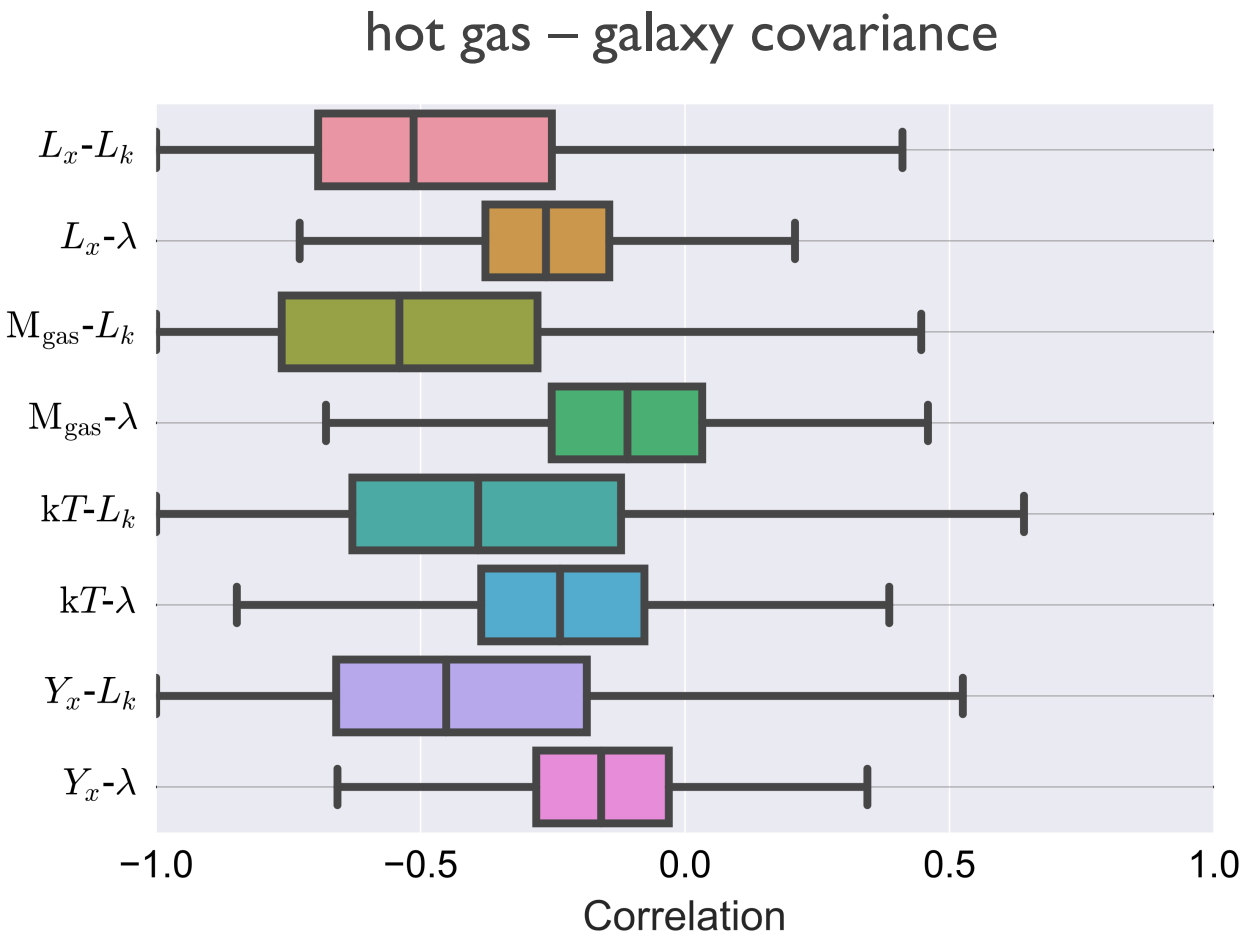

preliminary evidence for **anti-correlation** of hot and cold phase baryons! :)

supports ~closed box baryonic nature of high mass halos predicted by simulations

Dark Energy Survey
X-ray – optical scaling

Dark Energy Survey : year 4 operations underway

Study dark energy/cosmic acceleration with four techniques

+ Galaxy cluster counts and clustering
+ Galaxy power spectrum
+ Weak lensing / cosmic shear
+ SN Ia

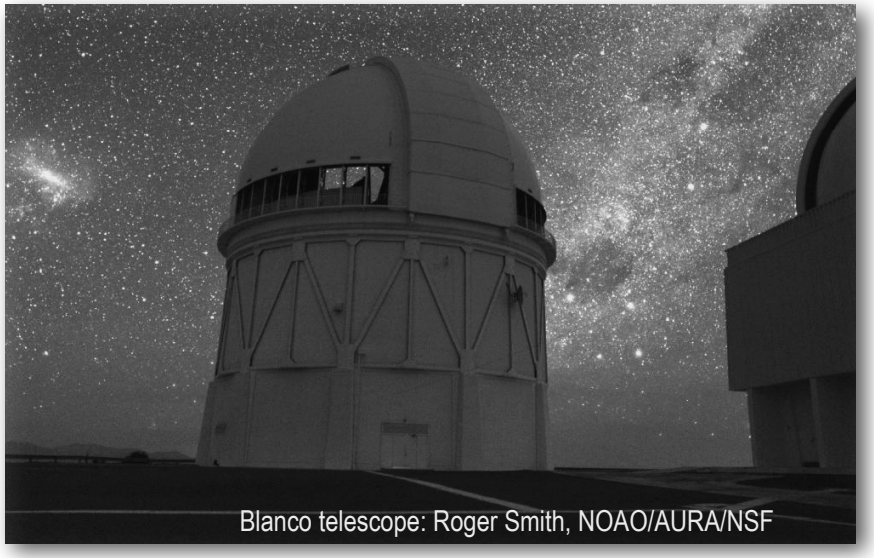

Two linked, multi-band optical surveys

5000 deg^2 *g r i z Y* bands to mag~23.5
Repeated observations of 30 deg^2 (10 SN fields)

Galaxy cluster science pubs

DES-SV redMaPPer catalog (Rykoff et al 2016)
Stacked weak lensing masses (Melchior et al 2016)
Six DES-SV strong lensing systems (Nord et al 2016)
Mass-richness for joint DES-SV+SPT sample (Saro et al 2015)

Associated multi-wavelength surveys

X-ray (Chandra + XMM)
South Pole Telescope
OzDES : 100 night spectroscopic follow-up (SN+)

rogue's gallery of DES-SV clusters - *many more where these came from!*

Images: Eli Rykoff (SLAC)

DES redMaPPer SVA1 cluster sample

Rykoff, Rozo + DES, 2016

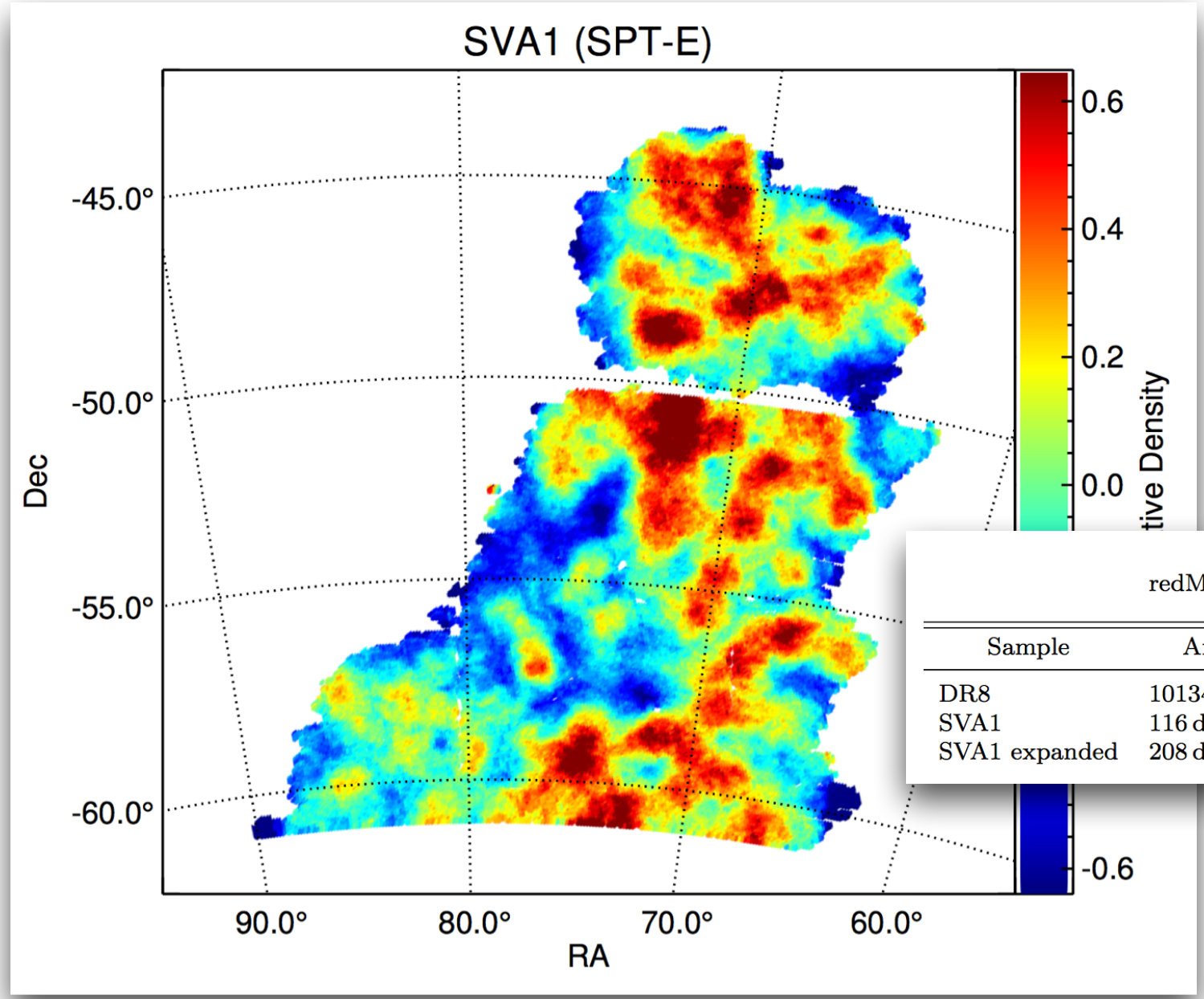

redMaPPer – a matched-filter likelihood method

small training set of spectroscopic redshifts sets the red sequence location

DES-SV samples

Table 1
redMaPPer Cluster Samples

Sample	Area	Redshift Range	No. of Cluster
DR8	10134 deg^2	$0.08 < z_\lambda < 0.6$	26308
SVA1	116 deg^2	$0.2 < z_\lambda < 0.9$	804
SVA1 expanded	208 deg^2	$0.2 < z_\lambda < 0.9$	1414

redMaPPer: DES-SVA1 + SDSS-DR8 cluster number densities

Rykoff, Rozo + DES, 2016

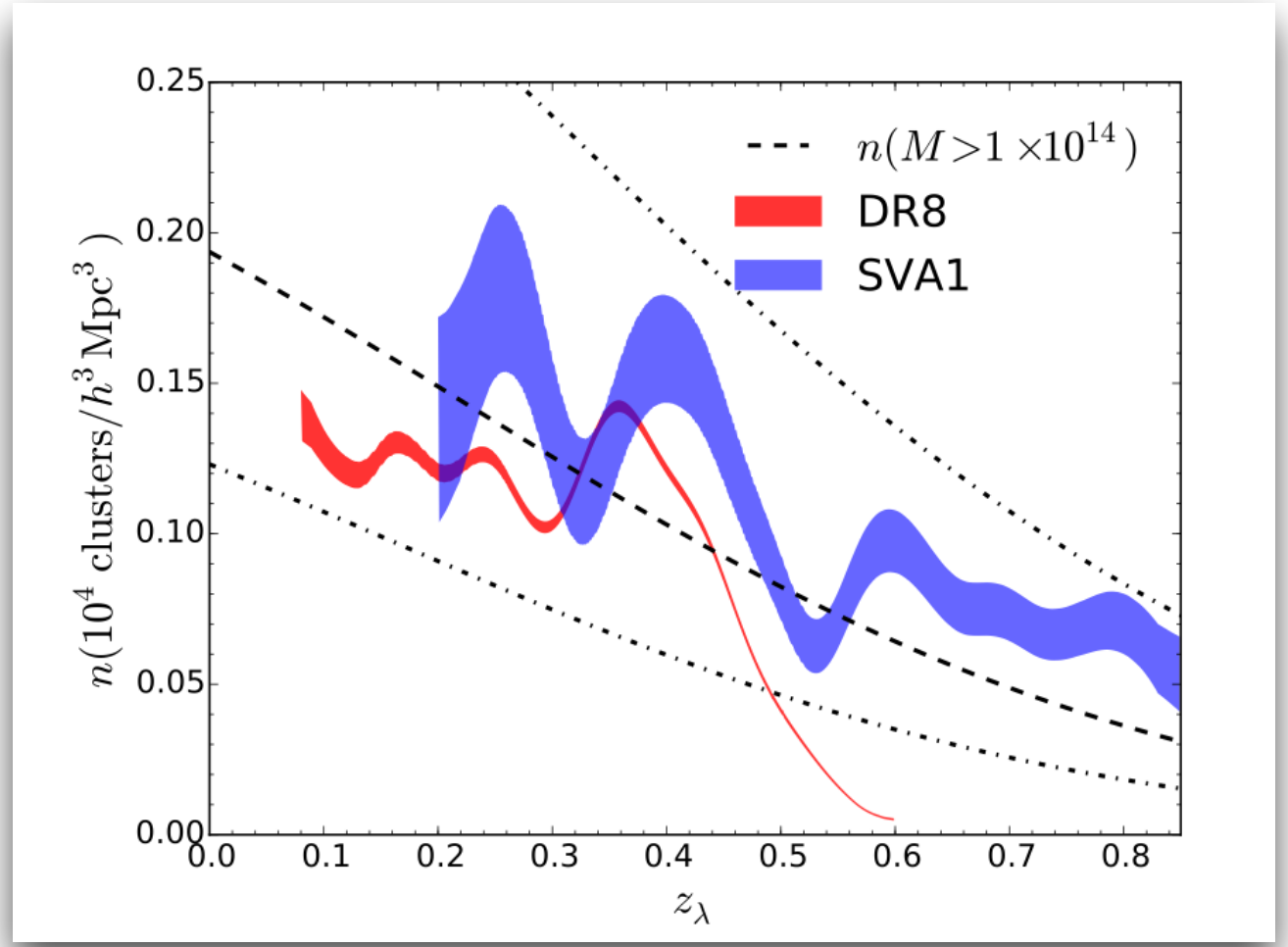

clusters with λ>20

~follow the space density of 10^{14} Msun halos in LCDM cosmology (not a design feature)

local variations from cosmic variance (DES) and Malmquist bias

DES redMaPPer + Chandra archive search

Hollowood + DES, in prep.

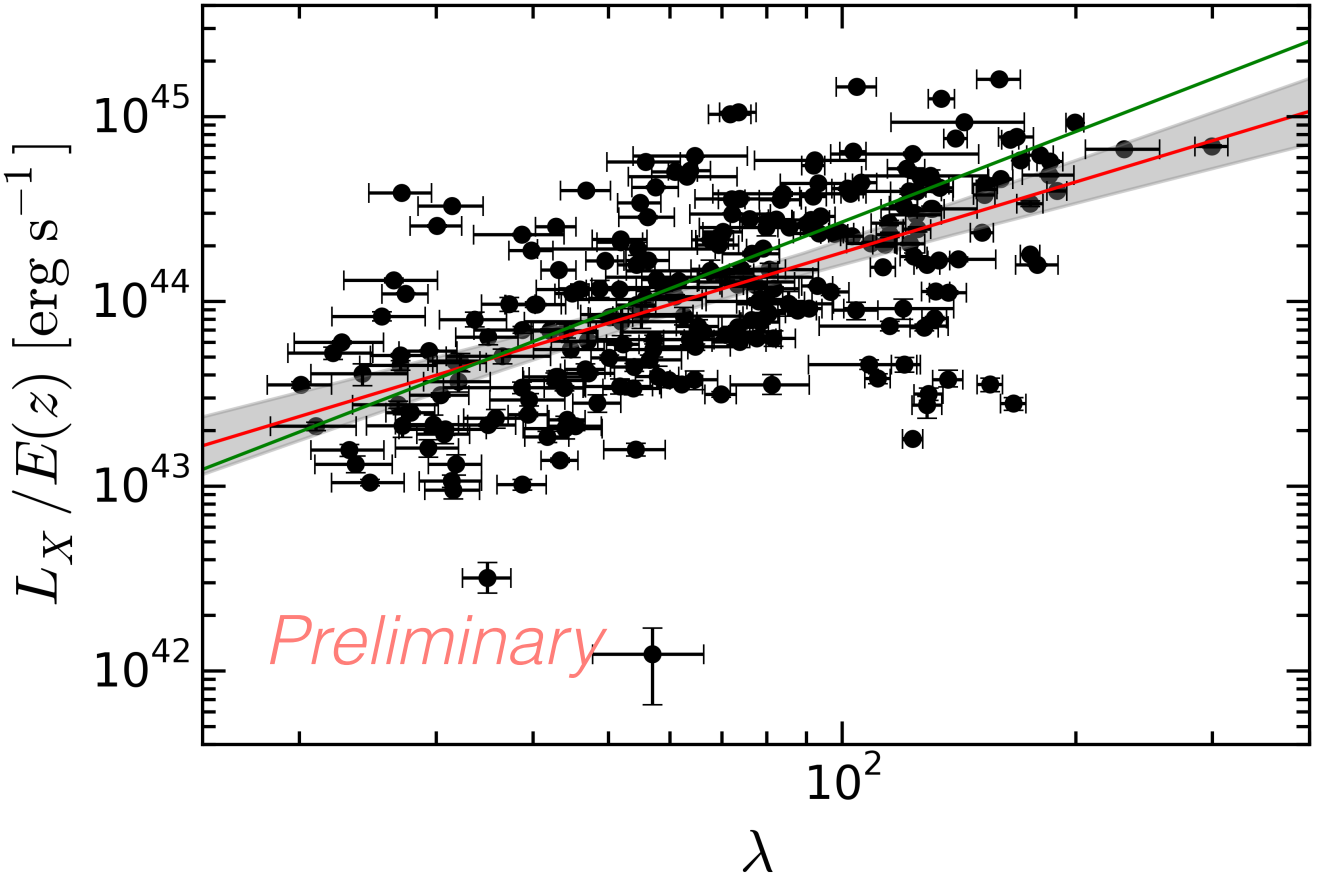

Tx-detected systems

Lx– λ

slope 1.27 ± 0.11

scatter 0.95 ± 0.05

DES redMaPPer + Chandra archive search

Hollowood + DES, in prep.

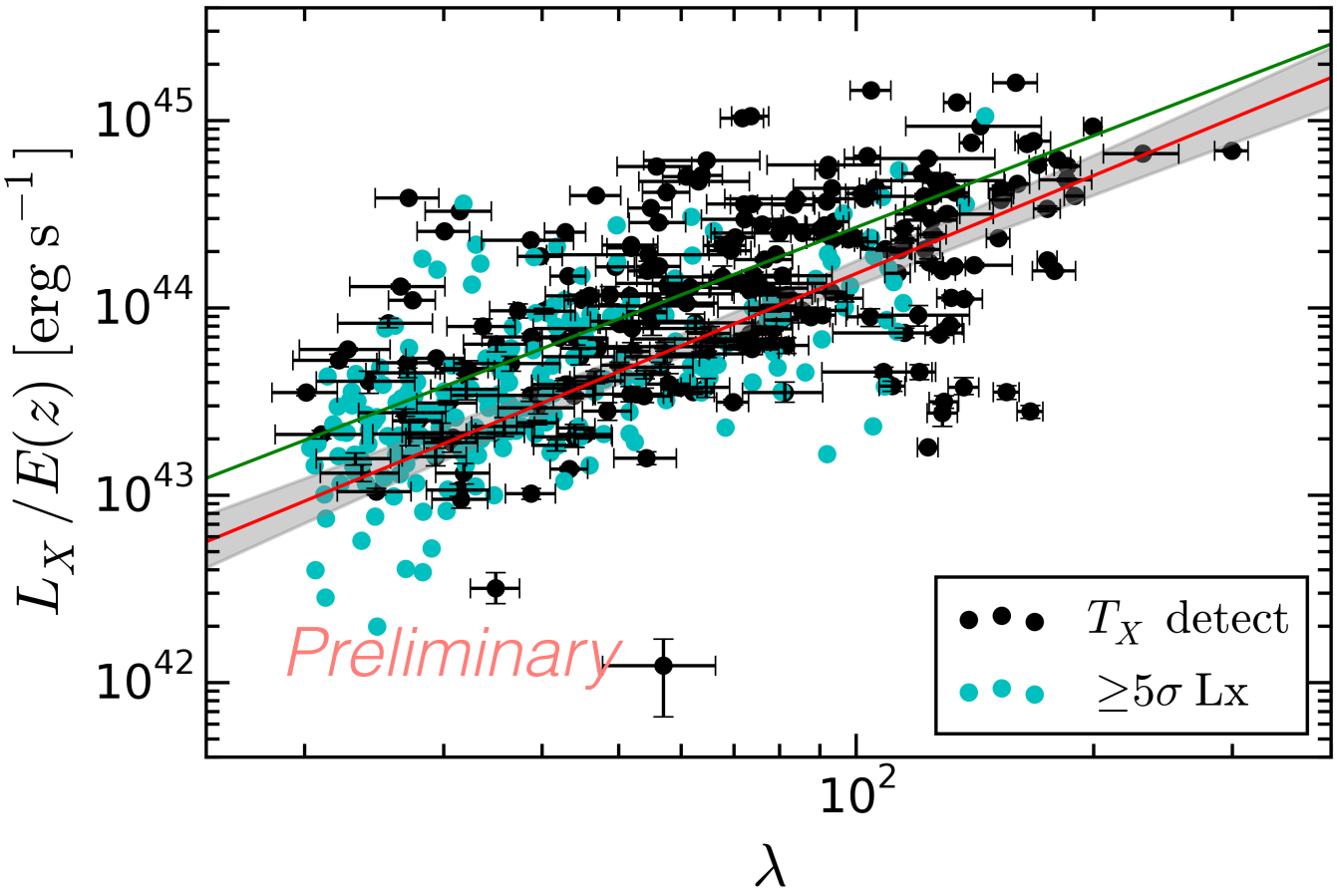

Tx-detected systems

Lx detected (5sigma)

Lx– λ

slope 1.74 ± 0.10

scatter 1.01 ± 0.05

DES redMaPPer + Chandra archive search

Hollowood + DES, in prep.

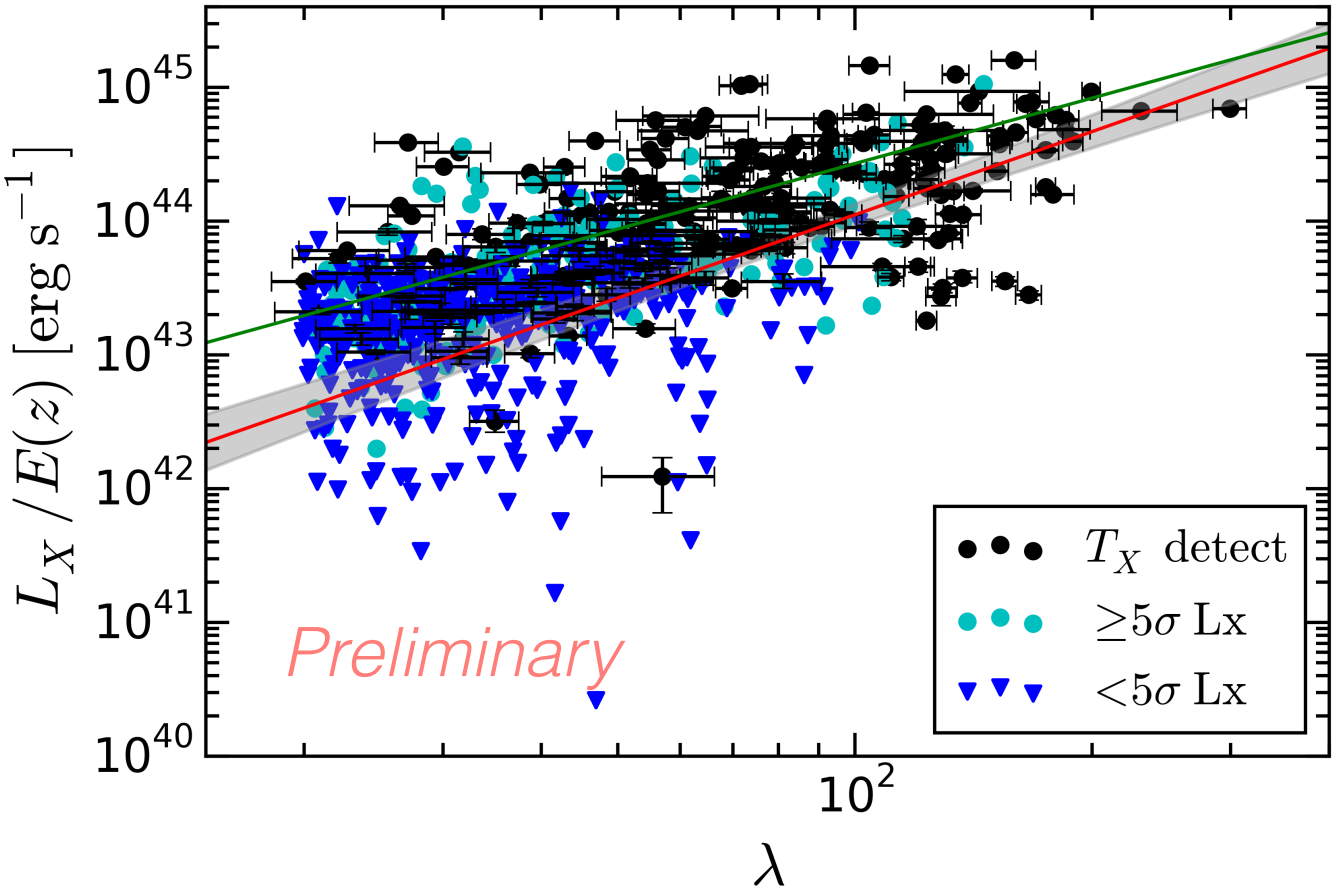

Tx-detected systems

Lx detected (5sigma)

Lx upper limit (<5sigma)

Lx– λ

slope 2.07 ± 0.13

scatter 1.26 ± 0.05

DES redMaPPer + Chandra archive search: residuals

Hollowood + DES, in prep.

Tx-detected

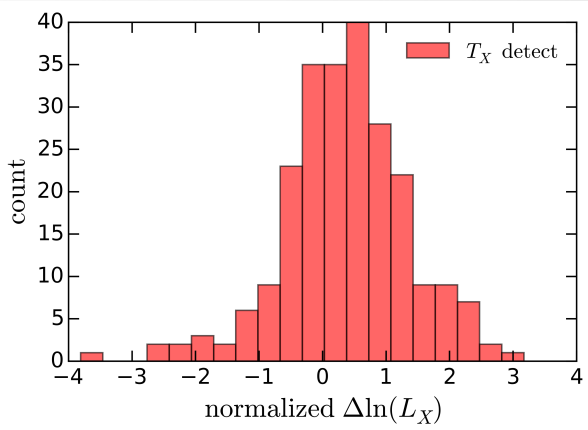

Lx detected

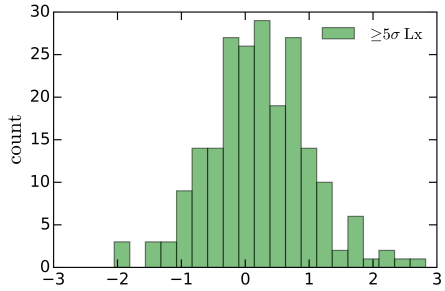

Lx upper limit

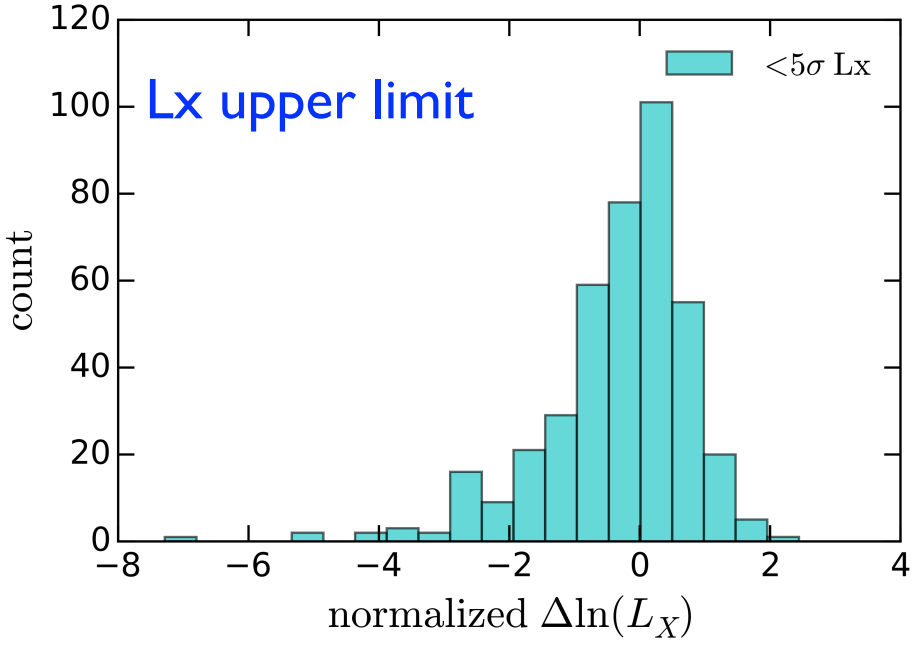

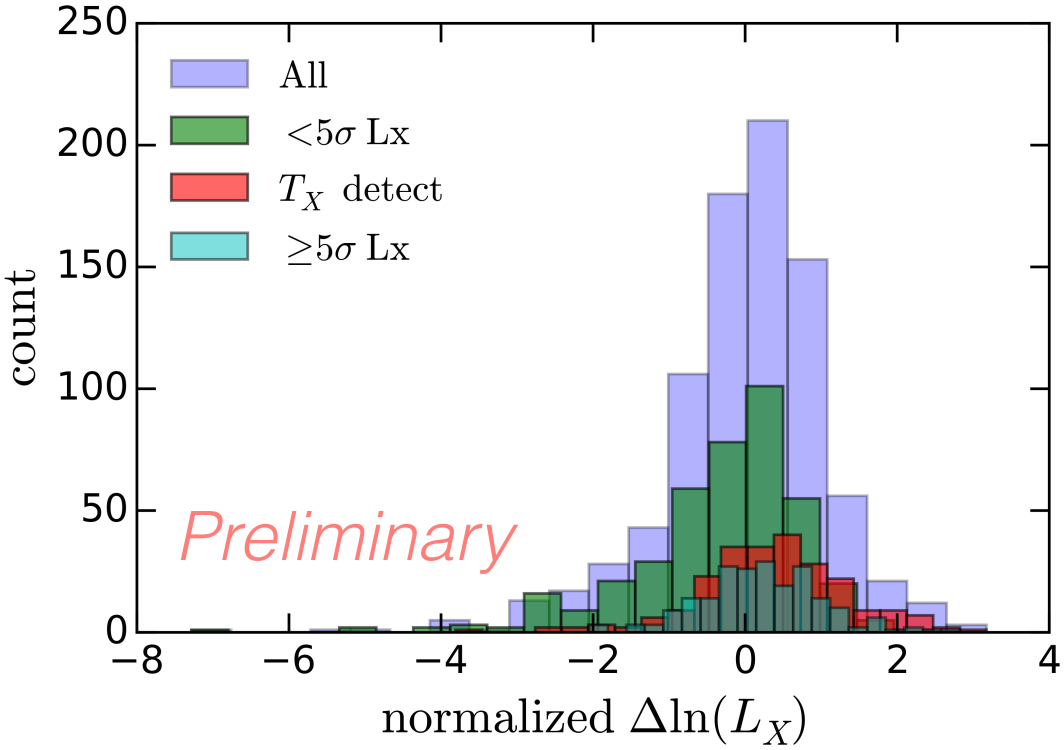

SDSS
X-ray – optical scaling

SDSS redMaPPer + XMM archive (XCS)

Bermeo, Romer, et al. (in prep.)

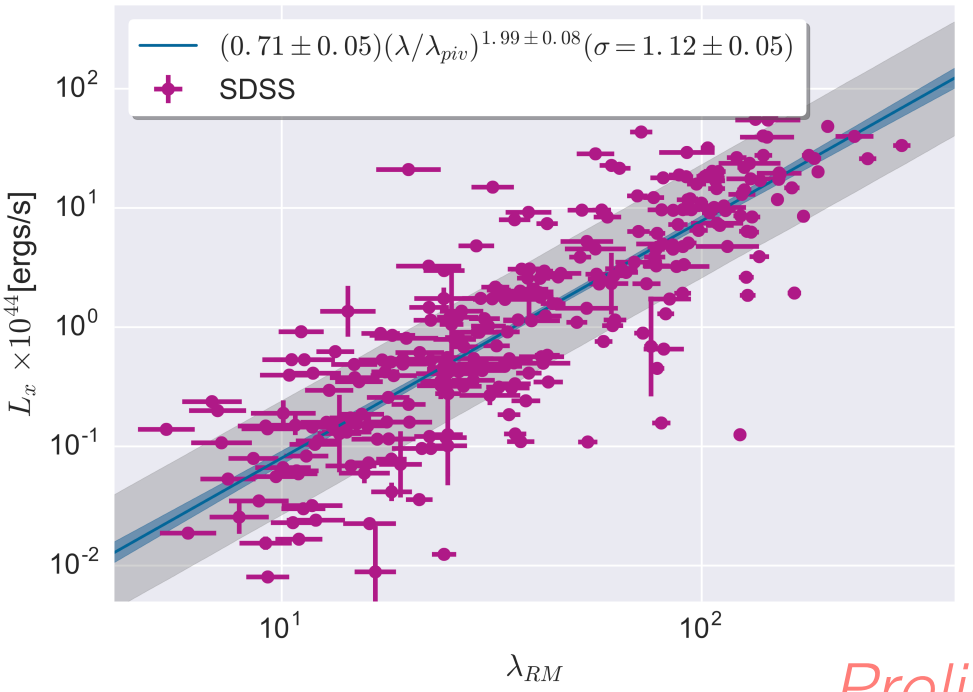

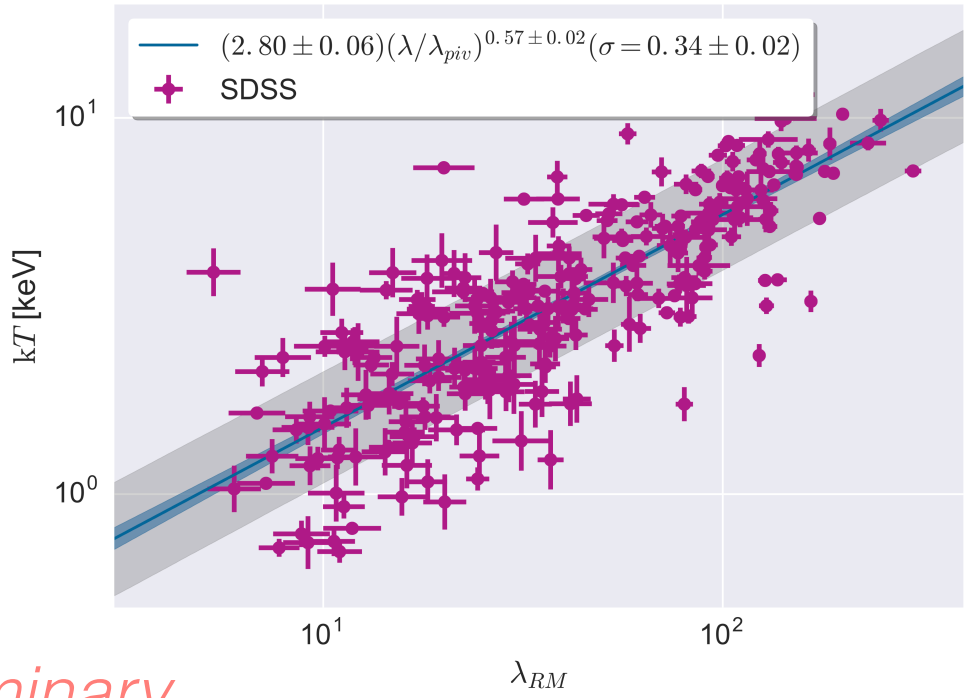

Preliminary

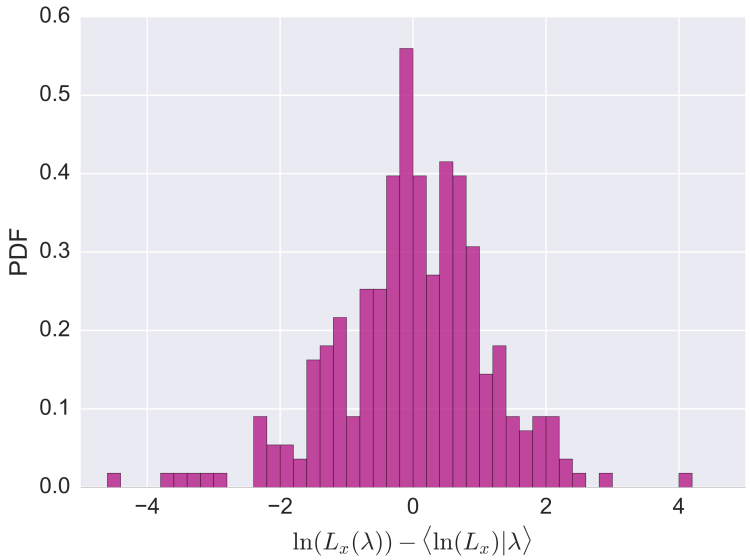

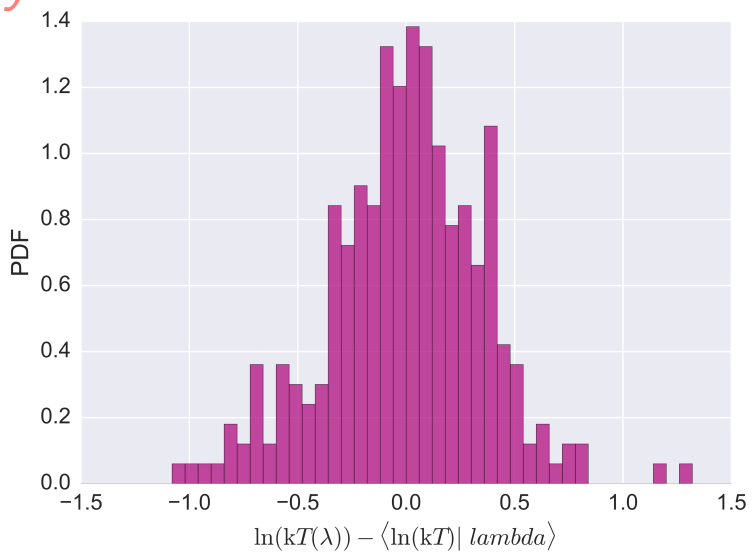

SDSS redMaPPer + XMM archive (XCS)

Bermeo, Romer, et al. (in prep.)

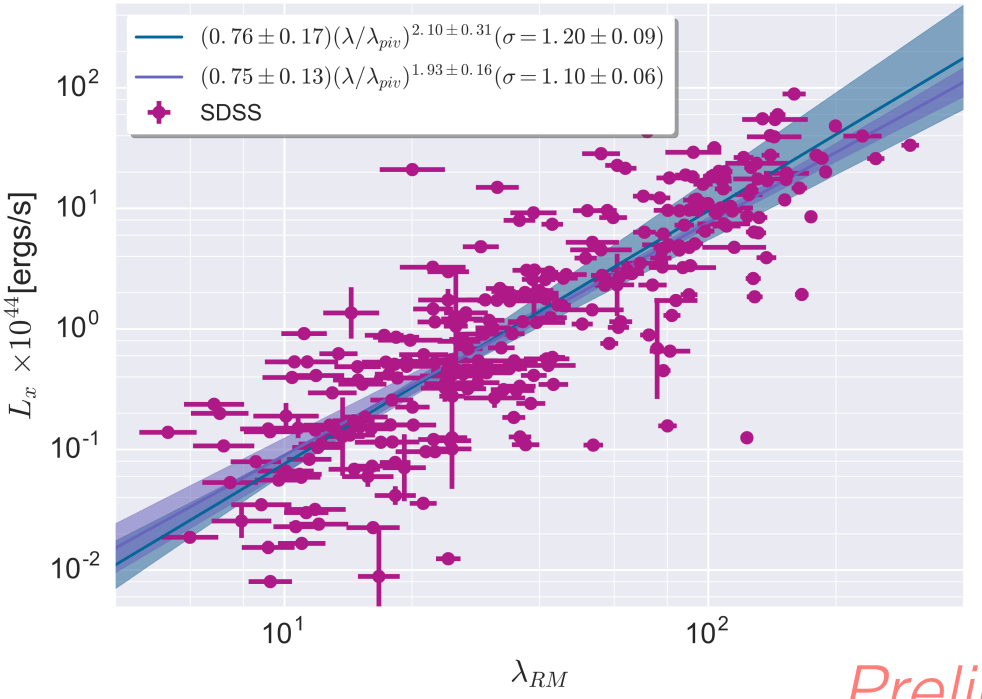

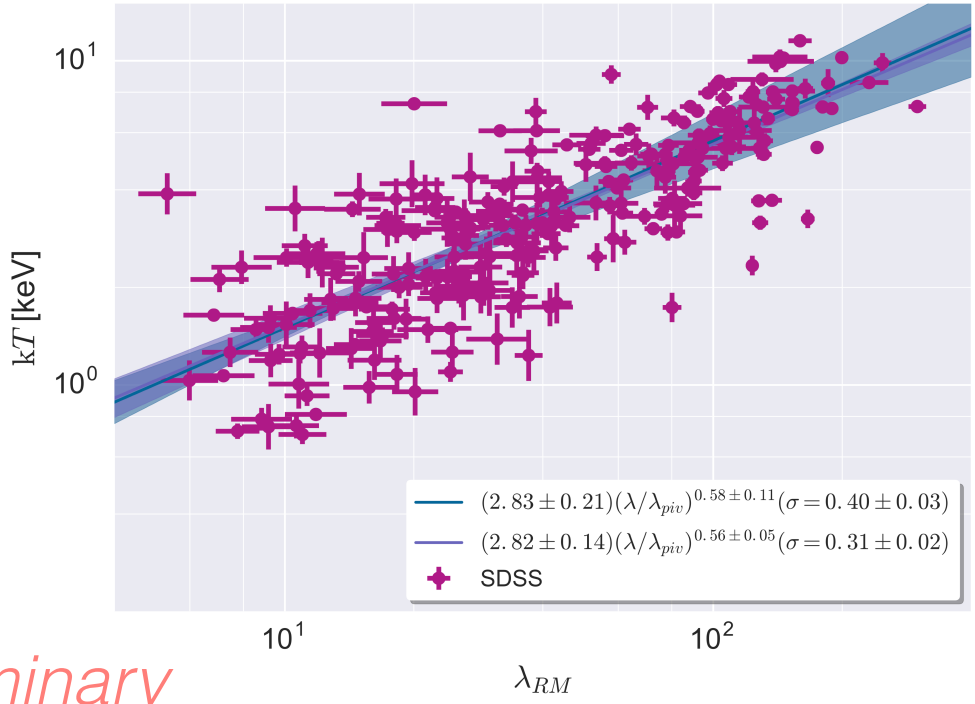

Preliminary

Lx– λ

groups, λ<30 : slope 2.10 ± 0.31
scatter 1.20 ± 0.09
clusters, λ≥30 : slope 1.93 ± 0.16
scatter 1.10 ± 0.06

Tx– λ

groups, λ<30 : slope 0.58 ± 0.11
scatter **0.40 ± 0.03**
clusters, λ≥30 : slope 0.56 ± 0.05
scatter **0.31 ± 0.02**

summary

A multi-wavelength statistical model of the group / cluster population?
Cool!

Looking forward to seeing how the measured slopes and scatter of observable properties can be combined to reveal underlying behaviors with respect to halo mass

$$\begin{aligned} \langle s_b | s_a \rangle_1 &= \pi_b + \alpha_b [\, \langle \mu | s_a \rangle_1 + \beta_1 \, r_{ab} \, \sigma_{\mu|a,1} \, \sigma_{\mu|b,1} \,] \\ \sigma^2_{b|a,1} &= \alpha_b^2 \, [\, \sigma^2_{\mu|a,1} + \sigma^2_{\mu|b,1} - 2 r_{ab} \, \sigma_{\mu|a,1} \sigma_{\mu|b,1} \,] \end{aligned}$$

The End